Motion Based Design of Cable-Stayed Bridges

by

Salvatore Di Bernardo

Laurea, Civil Engineering (1990) University of Rome, "La Sapienza"

Submitted to the Department of Civil and Environmental Engineering
in partial fulfillment of the requirements for the degree of

Master of Science in Civil and Environmental Engineering

at the

MASSACHUSETTS INSTITUTE OF TECHNOLOGY

June 1998

Author .....
Department of Civil and Environmental Engineering
May 8, 1998

Certified by .....
Jerome J. Connor
Professor
Thesis Supervisor

Accepted by .....
Joseph M. Sussman
Chairman, Department Committee on Graduate Students

Motion Based Design of Cable-stayed Bridges

by

Salvatore Di Bernardo

Submitted to the Department of Civil and Environmental Engineering
on May 8, 1998, in partial fulfillment of the
requirements for the degree of
Master of Science

Abstract

Recent increases in limit spans of cable-stayed bridges have highlighted the need for new concepts in analysis and design. The increased flexibility requires more theoretical studies on non-linear behavior and on dynamic analysis. Design also is more oriented to a performance-based approach: motion control is more important than strength analysis.

My main objective is to define what are the parameters to control in order to design structures that meet the performance requirements in terms of displacements, velocities and accelerations at particular points. My methodology is based on the definition of simplified methods for performance based design of cable-stayed bridges. The results of these methods, implemented on simulation models, are verified through comparison with the results of detailed finite element analyses. My approach is extended both to static and dynamic analysis.

The results are compared to those obtained by more traditional methods and show the effectiveness of this approach. The conclusion is that it is possible to rely on these simplified methods especially for conceptual design of cable-stayed bridges. Further evolutions are foreseen in the field of aeroelasticity and active control theories applied to long span civil structures.

Thesis Supervisor: Jerome J. Connor
Title: Professor

Acknowledgments

My deepest gratitude goes to my advisor Jerome J. Connor who guided me in the process of writing this thesis. Our talks have always been a great source of new ideas and have opened my mind towards the most advanced approaches to research and design.

I also feel profound gratitude to E. Sarah Slaughter for having supported and advised me during my stay at MIT. I have learned a lot from her enthusiastic approach to civil engineering.

MIT is a great place where to be and where to meet special people, as all my classmates are. I have had the opportunity of learning a lot of what is going on in the world and probably a great part of what will happen in the next future.

It has been a great experience of life I have had the pleasure of sharing with my wife Paola and little Matteo.

Contents

1 Introduction **13**

2 Simplified model for vertical loads **17**

2.1 Cables 18

2.2 Cable modeling in cable-stayed bridges 19

2.3 Application to the model 25

2.4 Plane finite element model 33

3 The spatial models **41**

3.1 Behavior under lateral loads 41

3.2 Description of the model 42

3.2.1 Characteristics of the structural elements 43

3.2.2 The finite element model 45

3.3 Linear elastic analysis 46

3.3.1 Modal analysis results 48

3.4 Non-linear formulation 51

4 Modeling of wind actions **55**

4.1 Wind action description 56

4.2 Wind actions as static loads 57

4.3 Dynamic effects of wind actions 58

4.3.1 Turbulence 58

4.3.2 Spectra used for structural design purpose 59

4.3.3 Vortex shedding 62
4.3.4 Torsional instability and flutter 63
4.3.5 Galloping and wind-rain instability 66
4.3.6 Buffeting by wind turbulence 67
4.4 Conclusion and remarks 67

5 Passive devices for motion control **71**
5.1 Tuned Mass Damper, description of behavior 72
5.2 Tuned Mass Damper theory for SDOF systems 73
5.2.1 Undamped primary systems 74
5.2.2 Damped primary systems 77
5.3 Extension to MDOF systems 77
5.3.1 Application to the cable-stayed bridge model 78

6 Active motion control systems **89**
6.1 Technological paradigms in long span bridge design 91
6.2 Technical description and background 91
6.3 Stage of development 93
6.4 Future potentiality 95

7 Conclusions **97**

List of Figures

2-1 Scheme of the central span 21
2-2 Bridge Plane Model 26
2-3 Variation of required vertical stiffness 28
2-4 Required area of cables for different values of stiffness 28
2-5 Vertical deflection of the central span 29
2-6 Rotation of the central span 29
2-7 Area of the cables - Minimum girder inertia 30
2-8 Areas of the cables - SemilLog graph 31
2-9 Obtained initial stiffness - Minimum girder inertia 31
2-10 Obtained initial stiffness - Maximum girder inertia 32
2-11 Comparison of the deflections due to vertical loads for different designs 35
2-12 Comparison of the normalized deflections due to vertical loads for different designs 35
2-13 Effects of the girder-tower constraints on the main span deflections . 36
2-14 Period for different vertical modes - Minimum inertia 36
2-15 Period for different vertical modes - Maximum inertia 37

3-1 Three dimensional model 47
3-2 Modes 1^{st} to 4^{th} 52
3-3 Modes 5^{th} to 8^{th} 53

4-1 Power spectral density functions variation with non-dimensional frequencies 60

4-2 Power spectral density functions variation with non-dimensional frequencies - log scale 60
4-3 Power spectral density functions variation with non-dimensional inverse frequencies 61

5-1 Design equivalent damping on the primary system - STMD 81
5-2 Required maximum dynamic amplification factor 81
5-3 Maximum dynamic amplification factor for the damper 82
5-4 Design damping ratio for the dampers - STMD 82
5-5 Design optimal tuning frequency 83
5-6 Midspan displacements, no TMD 83
5-7 Midspan displacement, single TMD 84
5-8 Midspan displacement, double TMD 84
5-9 Damper displacement, single TMD 85
5-10 Damper displacement, double TMD 85
5-11 Variations on midspan displacements no TMD, single and double TMD 86
5-12 Midspan displacement comparison between single and double TMD . 86
5-13 Damper vibrations relative to the primary system 87

6-1 Active control flowchart 90

List of Tables

1.1 Major cable-stayed bridges in the world 16

2.1 Model Geometry and Areas of Cables 38

2.2 Modal Frequencies - $I_{girder} = 0.54m^4$ 38

2.3 Modal Frequencies - $I_{girder} = 18.99m^4$ 39

3.1 Geometric Characteristics of Cables - $I_{girder} = 0.54m^4$ 44

3.2 Periods and maximum eigenvectors for each mode 50

Chapter 1

Introduction

Cable-stayed bridges are becoming very popular all over the world. Newer cable-stayed bridges have reached spans very close to 900 m (see Table 1.1);[1] and future evolution in the design will lead to further increases of the limit span. Although the strength of new materials allows this progress, the problems in the range of actual spans, and even more in superior spans come from the overall flexibility of the structural system. In fact, the span length increase results in a considerable increase in the displacements and the accelerations of the bridge under dead and live loads especially for the dynamic effects of traffic, earthquakes, and wind actions. As a consequence, the optimal design of cable-stayed bridges needs to be based more on the control of deflections, velocity, and accelerations than on the control of material resistance and strength.

This type of structures requires non-linear analysis, not only for dynamic actions but also for static loads. In fact, the cable itself has a non-linear behavior, as its axial stiffness is a function of the sag and of the tension [7]. Another non-linear effect comes from the behavior of bending elements subject to axial load. The typical beam column model can be applied both to the girder and the tower, as in both cases the stiffness depends on the level of compression of the member [8]. Second order effects are also related to the material non linearity such as the post-cracking behavior of

[1]From: Karoumi Raid, 'Dynamic Response of Cable-Stayed Bridges Subjected to Moving Vehicles', Licentiate Thesis, Dept. of Struct. Eng., Royal Institute of Technology.

concrete elements [19] or the post-yielding behavior of steel members. Many studies have been developed for the non-linear modeling of cable-stayed bridges both for the vertical loads [9] and for the dynamics actions of wind and earthquakes [24], [13], [14].

The main purpose of my research is to introduce motion based design [3] as an approach to cable-stayed bridge structural analysis and design. The objective of this approach is to define the values of the design parameters which minimize the displacements, velocities and accelerations of the system, in order to meet the serviceability requirements under the effects of static and dynamic loading. To fulfill this objective, I focus on the performance of sample models of three span cable-stayed bridges; the construction of these models is based both on the state of the art literature and on design patterns observed in existing projects. Through a motion based design approach I define the optimal stiffness and damping distribution throughout the system, the location and the dimension of motion control devices and finally the optimal overall structural arrangement of the system.

The conceptual design for vertical loads is based on a preliminary analysis of a simple model of a beam on an elastic foundation with constant stiffness [11]. This is the simplest way of representing the central span of a three span cable-stayed bridge. The purpose is to find an optimal distribution of the cables under the effect of the dead load. The effect of the cables' sag on the stiffness is introduced through the use of a tangent stiffness modulus, which, therefore, accounts for the non-linear behavior of the cables.

The main characteristics of the wind actions and their interactions with the bridge structure are briefly described in the fourth chapter, as a basis for the formulation of computational dynamic analysis. The objective of computational static and dynamic analyses for vertical and lateral load is to assess how effective are of passive and active damping or base isolation devices in limiting the dynamic response of the system to the required levels.

The areas of the cables that result from the simplified design approach are implemented in a three dimensional finite element model in ADINA [4]. I use this model to extract the fundamental modes and to perform a dynamic analysis of the forced

response due to wind actions. The ratio between the first mode period, which is a lateral mode, and the second lateral mode is around 2.3. The effectiveness of Tuned Mass Damper in the control of wind excitation is tested using the model.

The final chapter outlines the basics of an active system for the control of the aerodynamic excitation. It seems that this field will see a lot of improvement in the next year leading long-span bridge structures well beyond what are considered the actual limits.

Table 1.1: Major cable-stayed bridges in the world

Bridge name	Country	Center span (m)	Year of completion	Girder material
Tatara	Japan	890	1999	Steel
Pont de Normandie	France	856	1994	Steel
Yangpu	China	602	1993	Composite
Xupu	China	590	1996	Composite
Meiko Chuo	Japan	590	1997	Steel
Skarnsund	Norway	530	1991	Concrete
Tsurumi Tsubasa	Japan	510	1995	Steel
Oresund	Sweden	490	1999	Steel
Ikuchi	Japan	490	1991	Steel
Higashi Kobe	Japan	485	1994	Steel
Ting Kau	Hong Kong	475	1997	Steel
Annacis Island	Canada	465	1986	Composite
Yokohama Bay	Japan	460	1989	Steel
Second Hooghly	India	457	1992	Composite
Second Severn	England	456	1996	Composite
Dartford	England	450	1991	Composite
Rama IX	Thailand	450	1987	Steel
Chang Jiang Second	China	444	1995	Concrete
Barrios de Luna	Spain	440	1983	Concrete
Tonglin Cangjiang	China	432	1995	Concrete
Kap Shui Mun	Hong Kong	430	1997	Composite
Helgeland	Norway	425	1991	Concrete
Nanpu	China	423	1991	Composite
Hitsushijima	Japan	420	1988	Steel
Iwagurujima	Japan	420	1988	Steel
Yuanyang Han Jiang	China	414	1993	Concrete
Meiko-Nishi Ohashi	Japan	405	1986	Steel
St. Nazarine	France	404	1975	Steel
Elorn	France	400	1994	Concrete
Vigo-Rande	Spain	400	1978	Steel
Dame Point	USA	396	1989	Concrete
Baytown	USA	381	1995	Composite
Luling, Mississippi	USA	372	1982	Steel
Flehe, Duesseldorf	Germany	368	1979	Steel
Tjorn (new)	Sweden	366	1981	Steel
Sunshine Skyway	USA	366	1987	Concrete
Yamatogawa	Japan	355	1982	Steel
Neuenkamp	Germany	350	1970	Steel
Tempozan	Japan	350	1990	Steel
Glebe Island	Australia	345	1990	Concrete
ALRT Fraser	Canada	340	1985	Concrete
West Gate,	Australia	336	1974	Steel
Talmadge Memorial	USA	335	1990	Concrete
Rio Parana	Argentina	330	1978	Steel
Karnali	Nepal	325	1993	Composite
Kohlbrand	Germany	325	1974	Steel
Guadiana	Portugal	324	1991	Concrete
Kniebruecke	Germany	320	1969	Steel
Brotonne	France	320	1977	Concrete
Mezcala	Mexico	311	1993	Composite

Chapter 2

Simplified model for vertical loads

The overall behavior of cable-stayed bridges is highly complex; it depends on the interaction among different structural elements, the girder, the towers and the cables. The girder is supported by several inclined steel cables connected to one or more towers that transfer all the live and dead load action down to the soil. The cables carry only axial tension force, while the towers and the girder can resist bending as well as axial compression.

The behavior of an inclined cable is non-linear since the sag of the cable due to the dead load effects the internal tension. This is a source of non-linear behavior of the whole system. Similarly, the effect of axial deformation on the bending stiffness of beam-column elements introduces additional geometric non-linearity. Other nonlinear effects on the system are introduced by material non-linearity typical both of steel and reinforced concrete elements.

The main parameters governing the displacements, velocities, accelerations and the force distribution in a cable-stayed system with respect to vertical loads are:

1. The geometric proportion between the tower height and the girder central span.

2. The number and the configuration of the cables.

3. The type of connection between the towers and the girder.

4. The inertia of the girder and the towers.

The following observations on the relevance of these design characteristics are derived from parametric and sensitivity studies [15], [22]. It has been proved that the highest efficiency of the cables system is reached when the ratio between the towers' height, over the girder, and the central span is between 0.20 and 0.25. This is the ratio that minimizes the total weight of the cables. This is also the range that most of the existing bridges respect. Newer bridges have usually a large number of cables; this helps reducing the deformation and the bending moment of the girder. These criteria in the design of the tower and the cable setting result in great economical advantages, particularly for long span bridges.

Regarding the constraints scheme, a rigid connection of the girder to the tower greatly increases the moment at this joint, without a great benefit for the maximum moment at the center of the midspan. As a consequence, the choice of a continuous girder simply supported at the tower results in a more cost efficient design. Furthermore, in many cases this choice is also convenient for earthquake design as it shifts the natural period of the structure to a range where the seismic action is less significant.

A final remark on the overall setting of three span or multiple span cable-stayed bridges relates to the construction phase. In fact, most of the existing cable stayed bridges are symmetrical with respect to the towers and this is particularly advantageous to reduce the bending on the towers during the construction process, when the girder assembly proceeds by cantilever from the towers.

All of the above consideration will be taken into account when constructing the model for the simulations that follow. The preliminary analysis will focus on the optimal dimensioning for vertical loads, these loads on long span bridges are mostly dead loads.

2.1 Cables

The basic need is for a high-strength elastic material with high Young Modulus and good resistance to fatigue. In order to carry the heavy loads for a long life-time, strands are usually preferred to ropes in cable-stayed bridges. There are four different

strand configurations:

1. Helically-wound galvanized strands, The Ultimate Tensile Strength (UTS) is $670MPa$.[1], and Young Modulus (E_0)is $165,000MPa$, the pre-stressing limit is 0.55 UTS. The fatigue strength is low.

2. Parallel wire strands, UTS is $1,800MPa$ and Young Modulus is $190,000MPa$.

3. Strands of parallel wire cables, UTS is $1,600MPa$ and Young Modulus is $200,0000MPa$. Galvanized wire cables' UTS is $1,570MPa$ and Young Modulus is $190,000MPa$.

4. Locked coil strands, they have several layers of round wires, only the outer layer may be galvanized. UTS is $1,500MPa$ and the Young Modulus is $170,000MPa$, the pre-stressing limit is .55 UTS.

One of the basic requirements is to limit the pre-stress level in cables. Considering the great influence of dead loads on the overall loading of the structure, a limitation of $\sigma = 0.4\sigma_u$ on the cables' tension level under the effect of dead load seems reasonable.

2.2 Cable modeling in cable-stayed bridges

The primary function of the cables is to provide vertical stiffness to the girder. The simplest model of cable-stayed bridges that can be used for the preliminary design of cables is a beam on elastic foundation. According to the theory of beams on elastic foundations of stiffness k [11], the fundamental equation in the case of uniformly distributed load q is

$$EI\frac{d^4y}{dx^4} + ky = q \tag{2.1}$$

[1] $1MPa = 10^6 N/m^2$=14.245ksi

In the case of a beam simply supported at both edges[2] the solution of this equation, assuming k constant throughout the central span, gives the following expressions for the deflections, the rotations and the curvature:

$$y = \frac{q}{k}(1 - \frac{\cosh \lambda x \cos \lambda x\prime + \cosh \lambda x\prime \cos \lambda x}{\cosh \lambda l_c + \cos \lambda l_c}) \tag{2.2}$$

$$\theta = \frac{q\lambda}{k} \frac{\sinh \lambda x \cos \lambda x\prime + \cosh \lambda x \sin \lambda x\prime - \sinh \lambda x\prime \cos \lambda x - \cosh \lambda x\prime \sin \lambda x}{\cosh \lambda l_c + cos\lambda l_c} \tag{2.3}$$

$$\chi = \frac{q}{\sqrt{kEI}} \frac{sinh\lambda x \sin \lambda x\prime + \sinh \lambda x\prime \sin \lambda x}{\cosh \lambda l_c + \cos \lambda l_c} \tag{2.4}$$

where l_c is the span of the beam, x is the distance from the left edge, $x\prime = l_c - x$, and λ is defined as:

$$\lambda = \sqrt[4]{\frac{k}{4EI}} \tag{2.5}$$

These expressions are the solutions of the fundamental equation (2.1) of an elastic simply supported beam on elastic springs, when the inertia of the beam I and the spring stiffness k are constant.

Through these equations it is possible to design cables in such a way that a prescribed value of the vertical stiffness is obtained. For example, if the design requirement is to meet a serviceability constraint on the vertical deflection[3] of the midpoint of the central span under a certain load, the required value of k can be calculated through equation(2.2) where x and $x\prime$ are both equal to half the total span l_c (see Figure 2-1). The coefficient α represents the required limit of the ratio between the span l_c and the vertical displacement δ.

[2]A refinement comes from considering the stiffness of the flanking spans as rotational springs at the edges of the central span.

[3]Other constraints may be introduced on the rotations, or curvatures through equations (2.3)and (2.4).

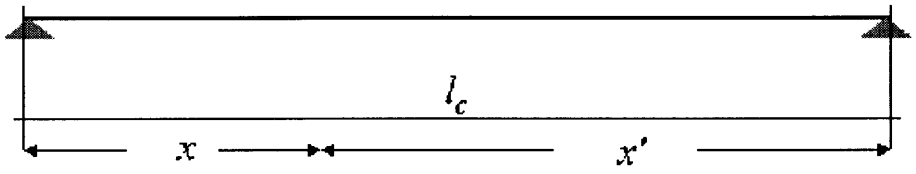

Figure 2-1: Scheme of the central span

$$\delta = \frac{l_c}{\alpha} \tag{2.6}$$

then taking the expression (2.2) of the solution in terms of vertical displacements and rewriting for $y = \delta$, and $x = x\prime = l_c/2$, the following is obtained:

$$k = \frac{q}{l_c/\alpha}[1 - 2\frac{\cosh(\lambda l_c/2)\cos(\lambda l_c/2)}{\cosh \lambda l_c + \cos \lambda l_c}]. \tag{2.7}$$

This equation together with the expression (2.5), which relates λ to k, gives the required value of k when the value of α is given together with the load and the inertia and modulus of the girder beam.

In the case of a multicable structure this model can give good results. To apply these equations to a cable-stayed structure the continuous geometric and inertial characteristics must be expressed in terms of the characteristics of a structure with a discrete distribution of stiffness. The following expression relates the uniformly

distributed stiffness to the equivalent characteristics concentrated in the cables:

$$K_n = \Delta x_n k \tag{2.8}$$

As a result, the stiffness K_n of the single cable can be obtained from the value of uniformly distributed stiffness. The subscript n stands for the n^{th} cable. The length of influence Δx_n is defined in the following way:

$$\Delta x_n = \frac{x_{n+1} + x_{n-1}}{2} \tag{2.9}$$

The vertical stiffness of the n^{th} cable of the central span can be expressed starting from its flexibility. It is expressed by superposition of three terms: first the flexibility of the cables of the central span, secondly the flexibility of the cables of the flanking spans, and lastly the contribution of the horizontal flexibility of the towers, ΔH_n^T is the horizontal displacement of the n^{th} cable at the tower. The complete expression by superposition is:

$$\Delta_n = \frac{x_n}{E_n A_n sin^2\theta_n cos\theta_n} + \frac{{x_n}^f}{E_n^f A_n^f cos^3{\theta_n}^f tan^2\theta_n} + \frac{\Delta H_n^T}{tan\theta_n} \tag{2.10}$$

where A_n is the area of the cross section and E_n the elastic modulus of the n^{th} cable, θ_n is the angle between the n^{th} cable and the girder, in which x_n is the distance of the cable anchoring at the girder from the point where girder meets the left tower. The superscript f indicates that variables are related to the flanking spans

In the following I have considered a three span cable-stayed bridge model, in which the cables are symmetrically arranged on the sides of the towers and the cross section of each cable is the same as its symmetrical. Therefore the following relations are true:

$$x_n = x_n^f; A_n = A_n^f; E_n = E_n^f; \theta_n = \theta_n^f \tag{2.11}$$

Furthermore the first three cables on the flanking spans are anchored to the piles,

in order to increase the stiffness of the longest cables. It follows that the only horizontal component of these cables at the tower is related to the elastic elongation of the anchored cables. The general expression for the vertical flexibility of the n^{th} cable is:

$$\Delta_n = \frac{2x_n}{E_n A_n sin^2\theta_n cos\theta_n} + \frac{\Delta H^T}{tan\theta_n} = \Delta_n^c + \Delta_n^T \tag{2.12}$$

where Δ_n^c and Δ_n^T are respectively the vertical flexibility of the girder's supports related to the cables and to the tower. The vertical stiffness of the n^{th} cable can be expressed by the following:

$$K_n = \frac{1}{\Delta_n} = \frac{1}{\Delta_n^c + \Delta_n^T} \tag{2.13}$$

$\Delta_n^T = 0$ if the cables are anchored on the flanking span.

Hence, the following formula can be used to express the area of the n^{th} cable as a function of the stiffness

$$A_n = \frac{K_n}{1 - K_n \Delta_n^T} \frac{2x_n}{E_n sin^2\theta_n cos\theta_n} \tag{2.14}$$

The value of the modulus E_n differs from the Young modulus E_0 of the cable itself. In fact, the influence of the sag on the modulus must be taken into account. The value of the modulus depends on the cable configuration in a non-linear way. An increase in the loading leads to a decrease in the sag, as a consequence, the cable stiffness increases. To synthesize this behavior the tangent stiffness modulus can be introduced. It is expressed by the Ernst formula [7] that relates the change in stiffness to the geometry of the cable and its tensile stress:

$$E_n = \frac{E_0}{1 + \gamma^2 x_n^2 E_0 / 12\sigma_n^3} \tag{2.15}$$

where γ is the specific weight of the cable, and σ_n is the tensile stress in the cable.

As stated above, a serviceability constraint on the vertical deflection of the mid-

point of the central span under a certain load gives the required value of k in the solution (2.2) of a beam on elastic foundation. From this required value of k the stiffness K_n of the single cable can be obtained. Once the required stiffness K_n of the cables is calculated, the area of the cables can be found using the following expression derived from equations (2.14), (2.15), and (2.8):

$$A_n = \frac{Kn}{E_0(1 - K_n\Delta_n^T)} \frac{2x_n}{\sin^2\theta_n \cos\theta_n} + \frac{Kn}{1 - K_n\Delta_n^T} \frac{\gamma^2}{12F_n^3} \frac{2{x_n}^3}{\sin^2\theta_n \cos\theta_n} A_n^3 \qquad (2.16)$$

F_n is the tensile force on the n^{th} cable.

This is an equation of third degree in the form $a * x^3 - x + b = 0$. It can be solved for real positive values A_n, the value of the two constants a and b are given by:

$$a = \frac{K_n}{1 - K_n\Delta_n^T} \frac{(\gamma x_n)^2}{12F_n^3} \frac{2x_n}{\sin^2\theta_n \cos\theta_n} \qquad (2.17)$$

$$b = \frac{K_n}{E_0(1 - K_n\Delta_n^T)} \frac{2x_n}{\sin^2\theta_n \cos\theta_n} \qquad (2.18)$$

In this way it is possible to obtain the areas of the cables through a performance requirement related to deformation and not to strength. In any case these areas must be tested for strength and resistance of material.

In a design based only on strength requirements, if forces are calculated as the cables were fixed support, the areas of the cables will be obtained by the following:

$$A_n = \frac{F_n}{\sigma_{all}} = \frac{P_n}{\sin\theta_n c_\sigma \sigma_{ult}} \qquad (2.19)$$

where c_σ is a coefficient that limit the level of stress in the cables to an allowable stress σ_{all} as a part of the ultimate strength.

2.3 Application to the model

To test all of the above considerations, I have first constructed a simple plane model of a bridge. The model bridge I have analyzed is a three span model with a central span of 600 m. The choice of this span relates to what was presented in the introduction. In fact, the actual trend in cable-stayed bridges construction shows that this dimension represents the upper boundary on the average economically feasible type of bridge. The objective of my work is to apply the simple approach presented above to step from conceptual design to more detailed design for a model of a long span bridge.

The dimension of the two flanking spans is 285 m, and is kept very close to half the central span; this to maintain the structure almost symmetrical with respect to the tower. The total height of the towers is 180 m (125m over the girder, around 20 percent of the central span). Each tower is fixed to the ground and support 36 cables, 18 per side; the cables are connected to the girder with 15 m spacing one from each other.

The cables layout is a mix of fan and harp pattern, as the cables are anchored in groups of three on the tower, with 5 m spacing. The lateral girders are pinned to the ground by hinges with a vertical constraint, these connections are distributed on the first three cables on the flanking span. The model is shown in Figure 2-2. Axial compression in the beams are neglected when forming the stiffness matrix and out of plane displacements are not allowed.

As explained in the last paragraph, the first objective is to dimension the cables in such a way that they can provide the beam with an uniform vertical stiffness. This stiffness based design is compared with a design based on a pure strength design criterion in which the area of each cable is dimensioned to support a longitudinal portion of the girder at a fixed level of tension.

The type of cables adopted in the conceptual design are be parallel wire strands with a Ultimate Tensile strength of $1,600 MPa$ and a Young modulus of $190,000 MPa$. It is assumed that the initial tension in the cables, should not exceed 40 percent of the UTS under the effect of the dead load (i.e.; $640 MPa$) this value agrees with that

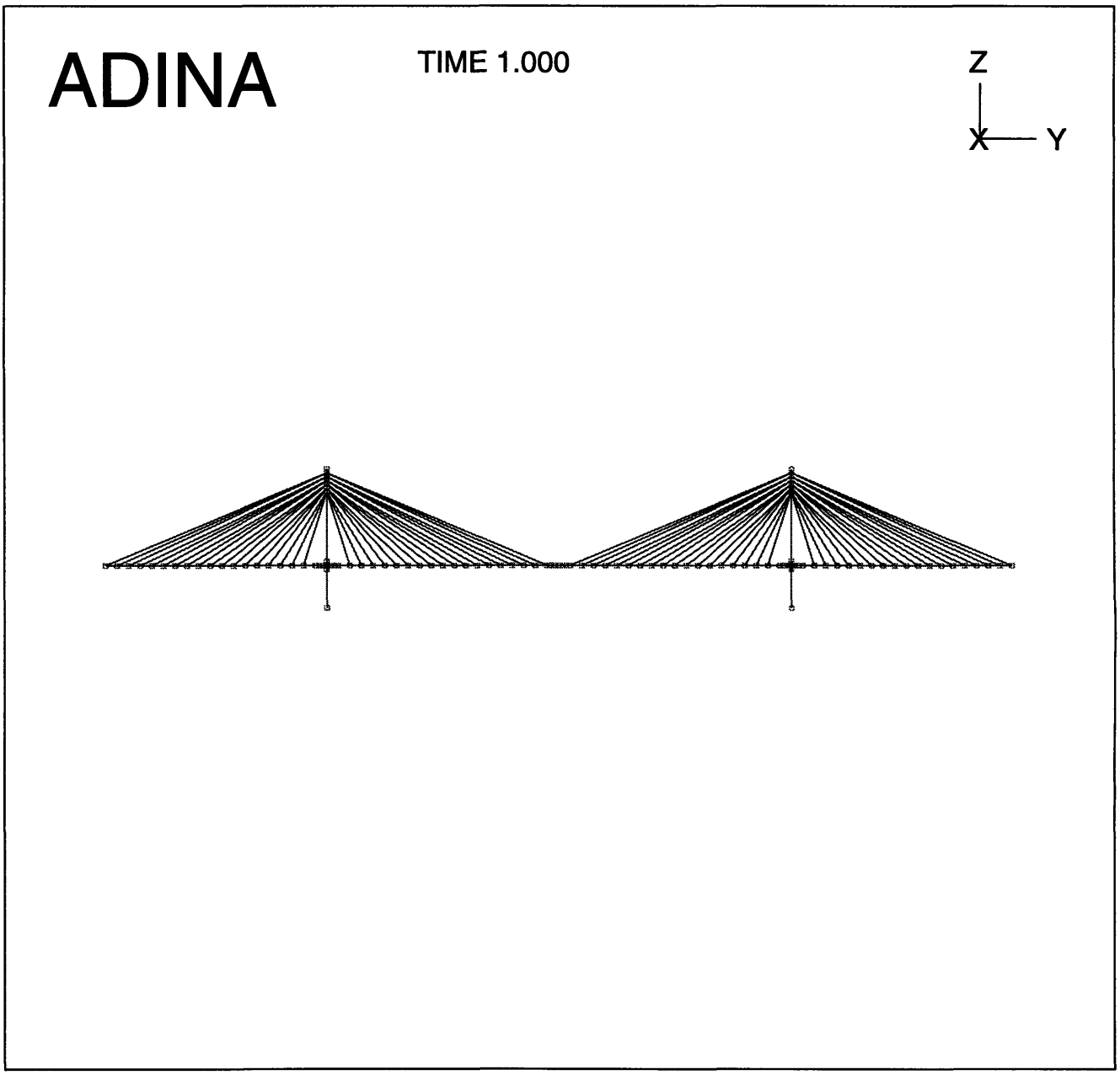

Figure 2-2: Bridge Plane Model

reported in recent literature [12], for a steel with an ultimate strength of $1,600MPa$.

The stiffness of the cables is directly related to the stress level; it decreases as the sag of the cable increases in the deformed shape due to its weight. A pseudo-linear analysis can be developed using a modified value of the Young modulus expressed as a function of the cable length and the level of tension according to (2.15), which can be used in a step by step analysis with an evaluation of tension in the different steps.

Even in linear elastic approximation the stiffness approach is oriented to conceptually design a structure with a determined value of the initial stiffness for the cables, in which the initial reduced modulus is taken into account. A purely strength approach will not respond to the requirements on the vertical deflections of the girder.

In the following figures are reported the graphs that describe the distribution of the area of cables along the central span obtained through the approach described in the latter paragraph, for specific value of α, q. In particular, a first analysis aimed to find out the variation of the required vertical stiffness with different value of the girder inertia.

The design requirement is the limitation of the midspan deflection to 1/300 of the central span, under a dead load of $100KN/m$. In particular, the analysis showed that a first minimum value of the required vertical stiffness lower than $k = 50KN/m^2$ (cables' stiffness) is related to an extremely low value of the girder inertia ($I_d = 0.54m^4$) see Figure 2-3. A direct proportionality is shown between the girder inertia and the required vertical stiffness towards a maximum value of $k = 57KN/m^2$ that corresponds to a relatively high value ($I = 18.99m^4$) of the girder inertia. A value of required cables' vertical stiffness equal to the one obtained for $I = 0.54m^4$ is obtained for $I = 79.99m^4$. All of these values lead to certain cables' areas, see Figure 2-4, in these values the reduced modulus is not taken into account.

Vertical displacements and rotations of the girder are plotted in the following Figures 2-5 and 2-6 for each value of the girder inertia and for half central span. In this case both displacements and rotations maximum values do not correspond to the midpoint of the central span, when the minimum inertia of the girder is adopted ($I_d = 0.54m^4$).

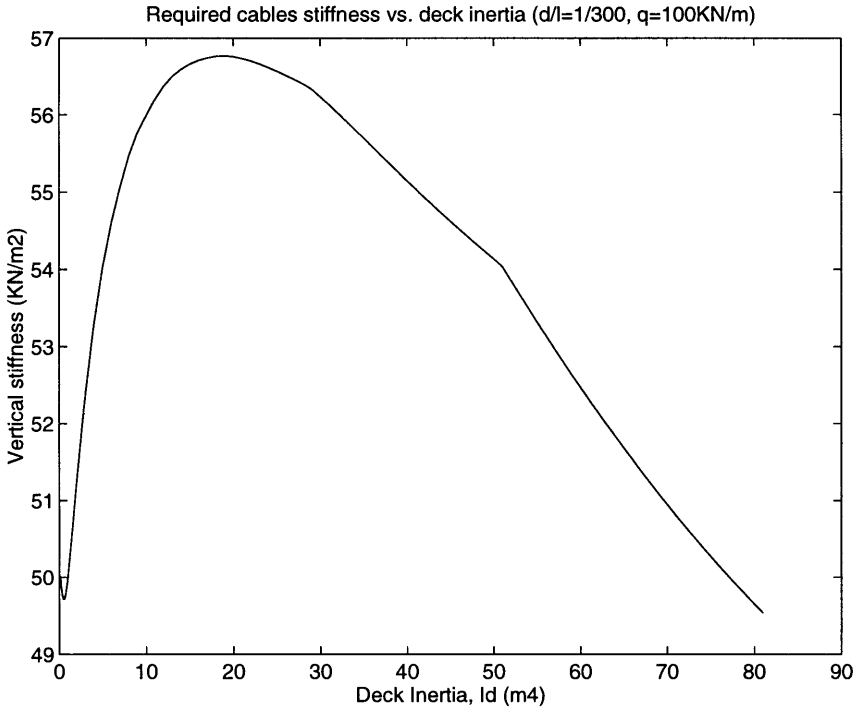

Figure 2-3: Variation of required vertical stiffness

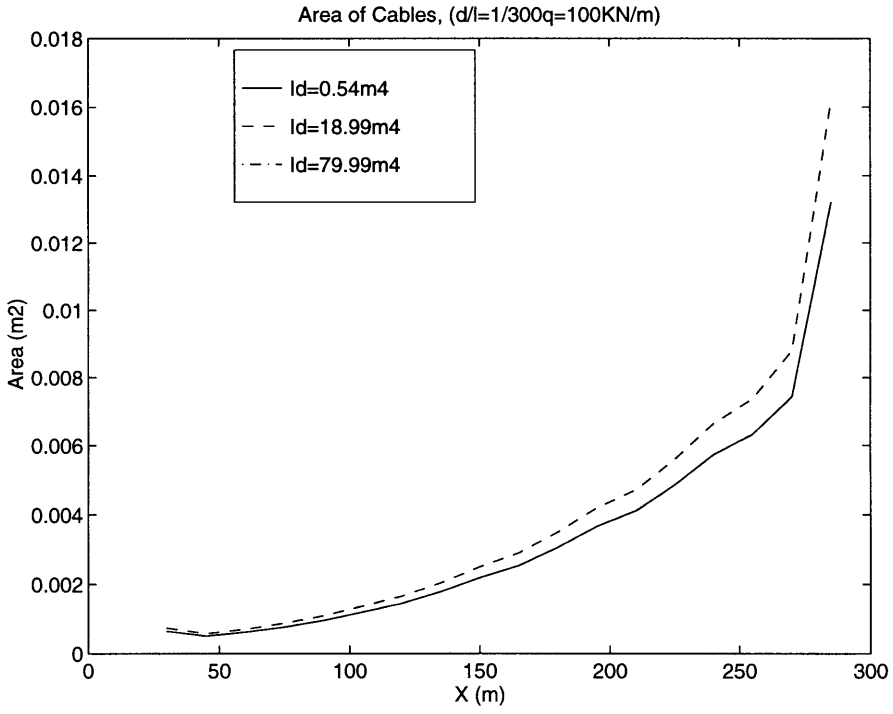

Figure 2-4: Required area of cables for different values of stiffness

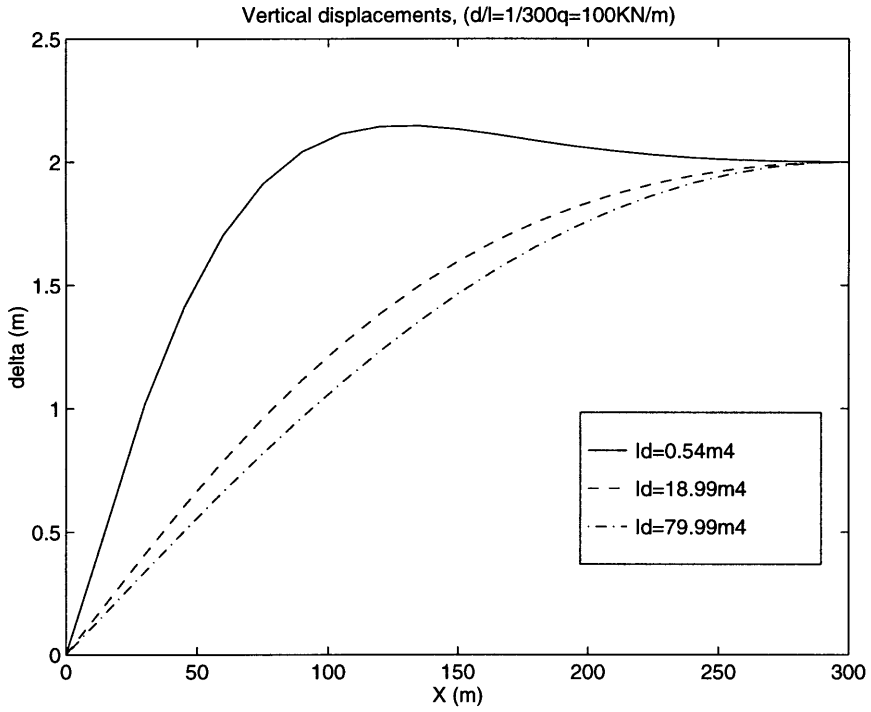

Figure 2-5: Vertical deflection of the central span

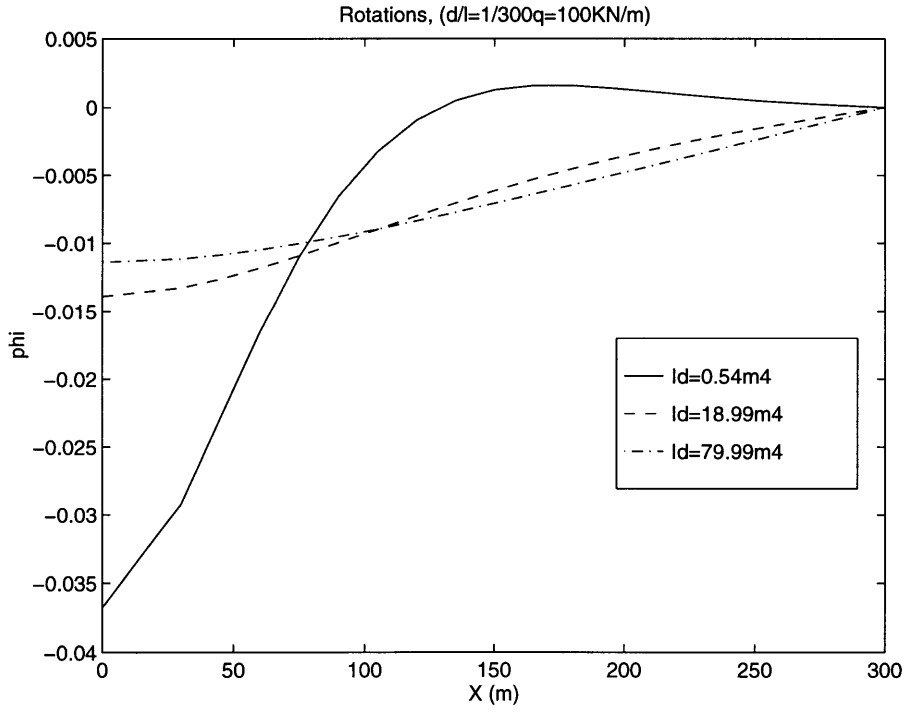

Figure 2-6: Rotation of the central span

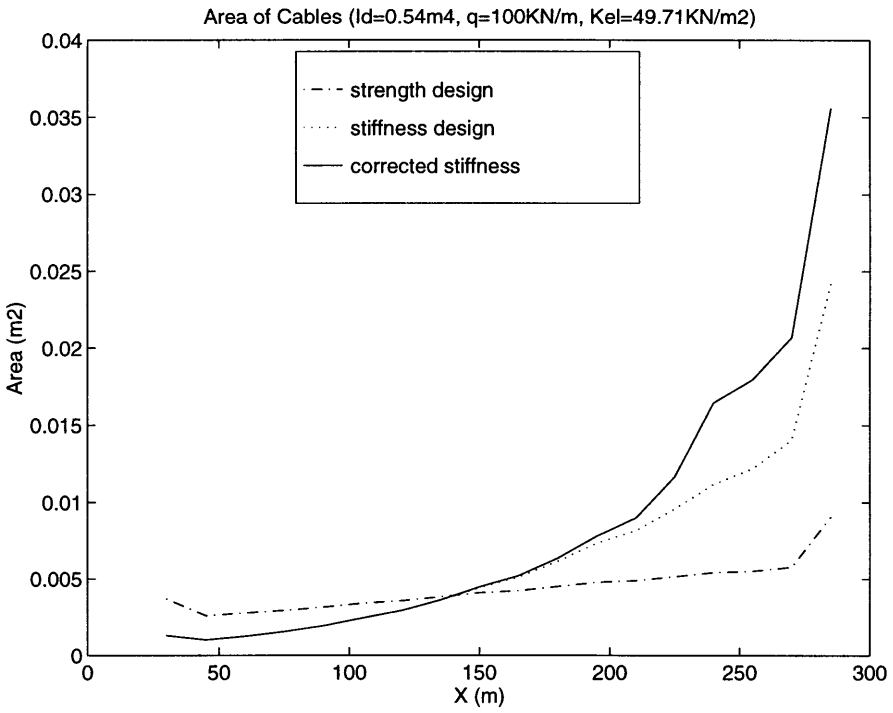

Figure 2-7: Area of the cables - Minimum girder inertia

The effective areas of cables that provide the required stiffness are determined. The values of areas obtained using equation (2.13), in which $E_n = E_0$, are compared with the values obtained considering the tangent modulus instead of the Young modulus. The variation of the values of the areas are reported in Figure 2-7 for the girder of lower inertia and compared to the area obtained with the strength design criterion, for $c_\sigma = 0.4$. It can be shown that the latter controls for the cables near the tower up to 150 m (a quarter of the central span) from the tower. Starting from this point stiffness design start to control. For the last four cables a correction to the initial force must be introduced to meet the required stiffness when solving equation (2.16) with respect to the area of cables.[4]

It is interesting to notice how the area distribution can be represented by a straight line in a semilogarithmic scale as shown in Figure 2-8. Figure 2-9 and Figure 2-10 show the initial vertical stiffness provided by the cable to the girder designed through the proposed conceptual approach.

[4]in order to obtain the required value of stiffness, as a combination of area and reduced modulus, the equation is solved by iteration with step increases of the force F_n

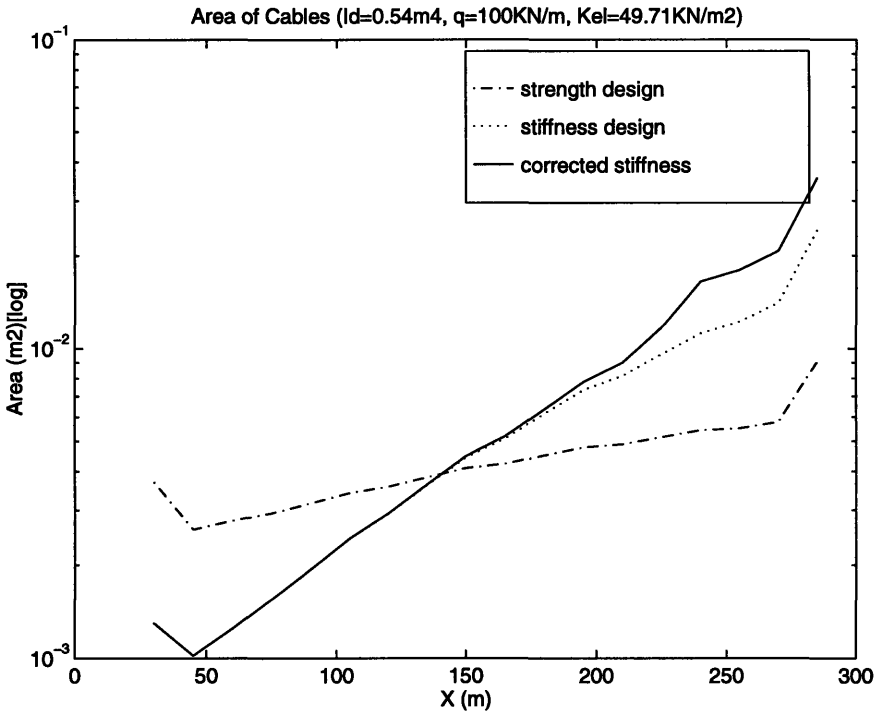

Figure 2-8: Areas of the cables - SemilLog graph

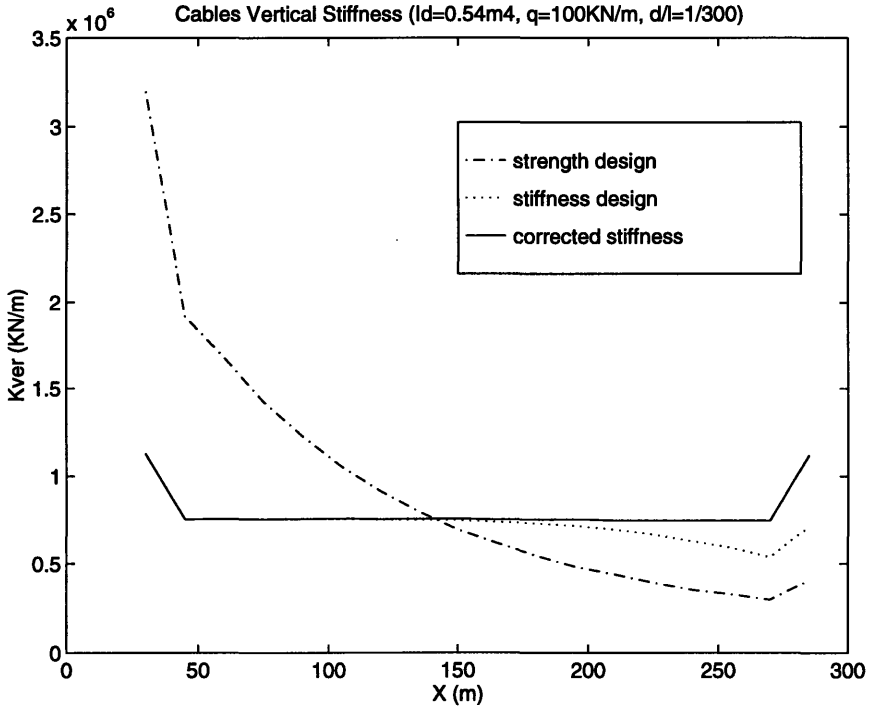

Figure 2-9: Obtained initial stiffness - Minimum girder inertia

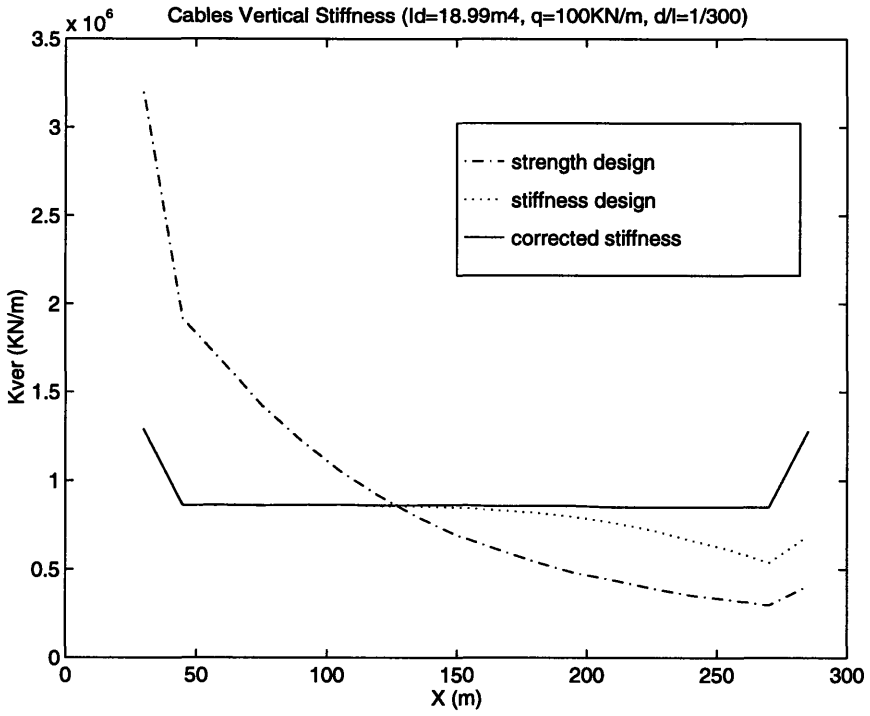

Figure 2-10: Obtained initial stiffness - Maximum girder inertia

Different performance based design conditions can be derived from the solutions in terms of rotations or curvature, deriving the value of the required k from equations (2.3) and (2.4).

To give a more detailed description of the values obtained, I report in Table 2.1 the areas of cables obtained with the pure strength criterion (A_{str}), the areas obtained with the stiffness criterion for minimum inertia (A_{ser}^{min}), and for maximum inertia (A_{ser}^{max}). These values of the areas include the correction for stiffness decay, obtained by pre-stressing the cables. D is the horizontal projection of the cable length, H is the height of the cable-tower joint from the girder, L is the length of the cable. The cables are numbered from 1 to 18 ideally starting from the tower and moving away from it for each group of cables. As the model is a plane model and the girder is a simple beam, in the same way the cables are concentrated in a single one no matter what is the real transversal configuration.

2.4 Plane finite element model

I have constructed a finite element model in which the values of cables' areas obtained by the above analyses were implemented. As a first step, the three different approaches to the design of the areas of the cables were compared. In one case the constant girder inertia of $I = 0.54m^4$, which is the value of girder inertia that minimize the area of cables, was used. For this value of the girder inertia, I have calculated the vertical deflections along the central span for an uniformly distributed vertical load for the arrangements of cables areas obtained through three different design approaches. In particular, I have considered the areas obtained by strength design, and by both stiffness and corrected stiffness design.[5].

The vertical deflections are reported in Figure 2-11 in which they are compared with the graph representing the mathematical solution of the beam on elastic foundation. The deflections of the system designed with a strength-based approach differ from the ones designed with a stiffness-based design approach. In particular, the maximum value is more than twice of the stiffness-based design value. By contrast, the values of the deflections obtained with the stiffness-based approaches are both very close to the ones calculated for the beam on an elastic foundation.

Other insights come from the normalized graphs of Figure 2-12, in it is easier to focus on the shape of the deflections along the girder. The figures show that the normalized deflection of the model in which cables are designed through a stiffness design that include pre-stress is very close to the one calculated through the solution of the beam on elastic foundation. In strength-based design the rate of growth of vertical displacements along the girder is very high. This is an undesirable behavior for a bridge structure whose serviceability strongly depends on the differential vertical displacement between adjacent points.

The conclusion is that the stiffness-based approach is reliable for conceptual design of cable-stayed systems. It gives the opportunity to better control the performance

[5]In the corrected stiffness design E_n is implemented as the tangent modulus and includes the application of pre-stress in the four cables closer to midspan on both sides of the central point

of the system under vertical loads in terms of displacement requirements. The results obtained for the response of the system through finite element analysis strictly correspond to the those that are obtained using the mathematical formulation based on the theory of beams on elastic foundations.

In the simplified model used in the stiffness-based design method I have modeled the central span as hinged at its edge neglecting the effect of the eventual continuity with the flanking span or with the tower. To assess the influence on the girder's displacements of the constraints at the beam edges I have used the finite element model. Figure 2-13 shows that, in the case of low girder inertia, the difference between the case in which the beam is hinged at its extremes and the case of tower-girder continuity is minimal and affects only the part of the central span that is closer to the tower itself. The case of continuity with the flanking span would be in between these two cases. As a consequence, having considered the beam as simply supported at its edges has not introduced an error in the stiffness-based design model.

In the following Table 2.2 the modal frequencies of the first ten mode of the plane model are reported. In particular, the model in which the cables were designed for strength(A_{str}) is compared with the model for which the areas of cables were designed for serviceability(A_{ser}).

In a similar way Table 2.3 reports the first ten modal frequencies of a plane model with a longitudinal girder inertia of $I = 18.99m^4$, which corresponds to the maximum required vertical stiffness for the cables. The frequencies reported correspond to the model in which the cables were designed for strength(A_{str})and to the model for which the areas of cables were designed for serviceability(A_{ser}).

The following figures show the shape of the first six modes in a sample case. It can be noticed that moving towards a design of cables for serviceability constraints, the model structure shows higher natural frequencies. The stiffness of the model increases; the difference is more relevant for lower values of the girder's inertia.

This can be better noticed when looking at the following figures (Figure 2-14 and Figure 2-15) that represent the natural periods of the different modes of vibration of the models and compare once again the strength design with the stiffness design.

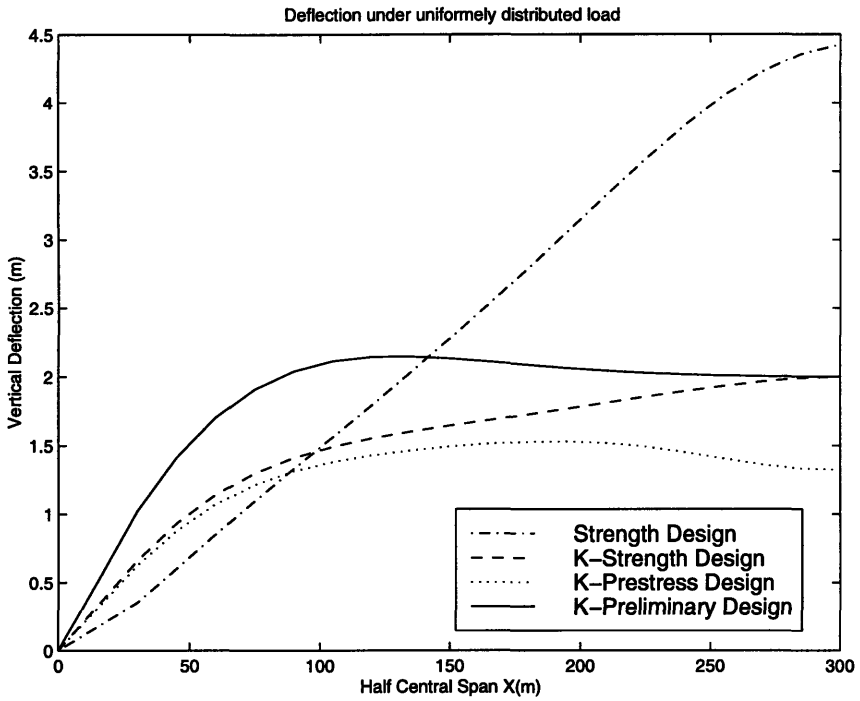

Figure 2-11: Comparison of the deflections due to vertical loads for different designs

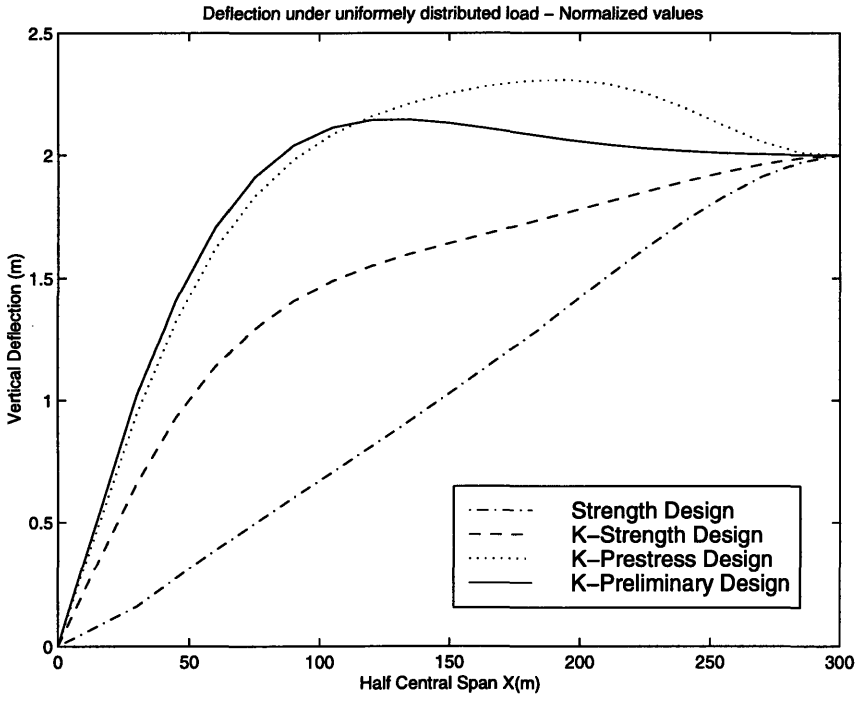

Figure 2-12: Comparison of the normalized deflections due to vertical loads for different designs

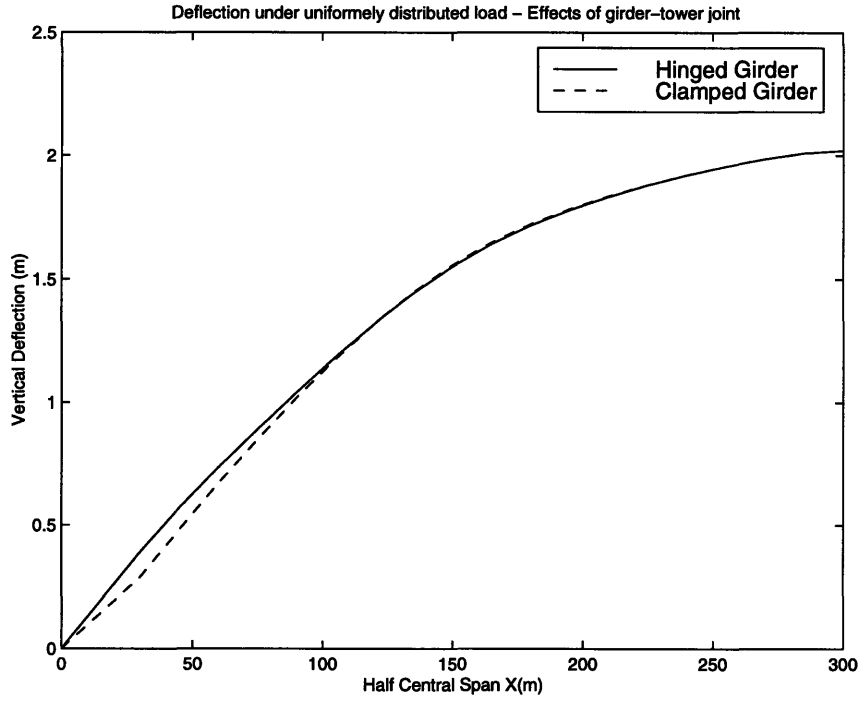

Figure 2-13: Effects of the girder-tower constraints on the main span deflections

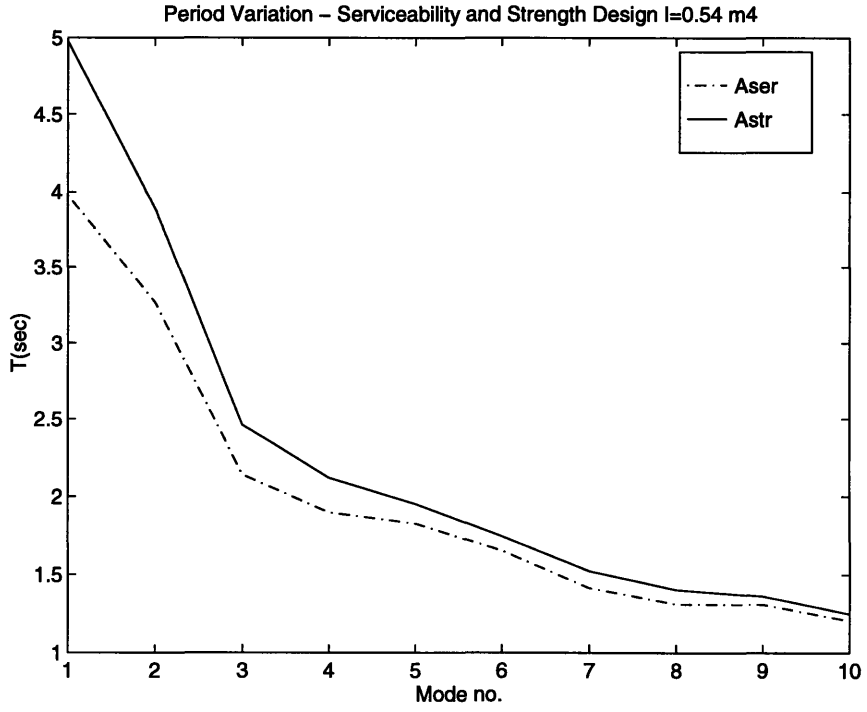

Figure 2-14: Period for different vertical modes - Minimum inertia

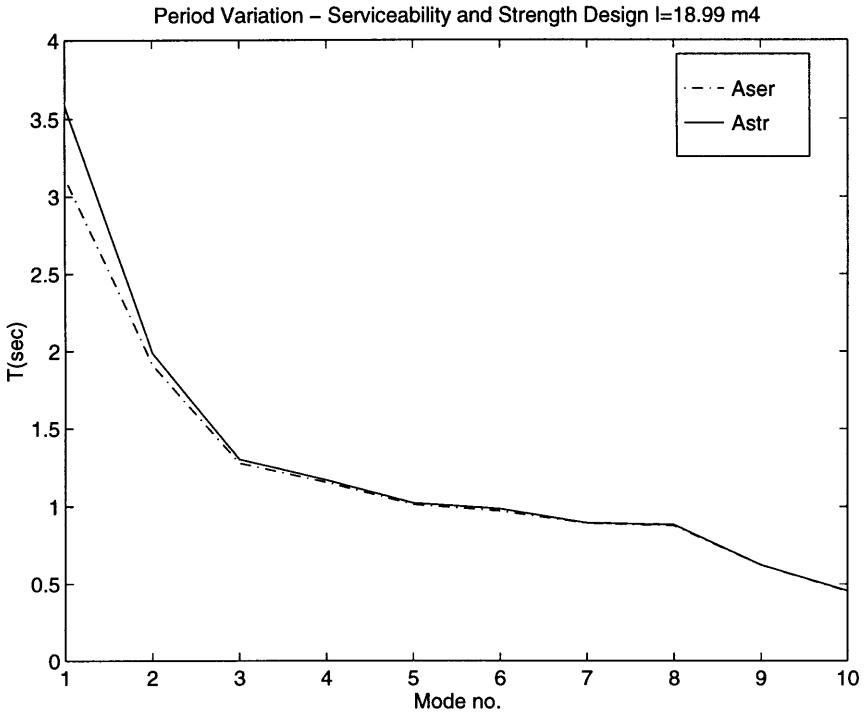

Figure 2-15: Period for different vertical modes - Maximum inertia

In conclusion, this simple model based on the solution of the beam on elastic foundation, gives good results when used to design the area of cables in order to make the structure meet a displacement requirement. This can be obtained through the solution of equation (2.16) that includes the effects of non linearity of the cables.

Table 2.1: Model Geometry and Areas of Cables

cable no.	D m	H m	L m	A_{str} cm^2	A_{ser}^{min} cm^2	A_{ser}^{max} cm^2
1	30	95	100	36.87	36.87	36.87
2	45	95	105	25.93	25.93	25.93
3	60	95	112	27.72	27.72	27.72
4	75	100	125	29.30	29.30	29.30
5	90	100	135	31.53	31.53	31.53
6	105	100	145	33.98	33.98	33.98
7	120	105	159	35.59	35.59	35.59
8	135	105	171	38.18	38.18	41.51
9	150	105	183	40.87	44.69	51.40
10	165	110	198	42.25	51.84	59.83
11	180	110	211	44.95	63.35	73.78
12	195	110	224	47.70	77.80	92.41
13	210	115	239	48.80	89.79	110.99
14	225	115	253	51.50	116.81	160.94
15	240	115	266	54.24	164.65	188.02
16	255	120	282	55.04	179.58	205.07
17	270	120	295	57.71	206.94	236.31
18	285	120	309	90.60	355.85	406.36

Table 2.2: Modal Frequencies - $I_{girder} = 0.54m^4$

MODE No.	$f(Astr)sec^{-1}$	$f(Aser)sec^{-1}$
1	0.201	0.251
2	0.257	0.306
3	0.407	0.468
4	0.472	0.527
5	0.513	0.548
6	0.573	0.605
7	0.657	0.708
8	0.713	0.763
9	0.734	0.764
10	0.800	0.830

Table 2.3: Modal Frequencies - $I_{girder} = 18.99m^4$

MODE No.	$f(A_{str})sec^{-1}$	$f(A_{ser})sec^{-1}$
1	0.279	0.320
2	0.503	0.523
3	0.769	0.783
4	0.855	0.867
5	0.978	0.988
6	1.015	1.029
7	1.117	1.119
8	1.131	1.140
9	1.600	1.604
10	2.191	2.210

Chapter 3

The spatial models

3.1 Behavior under lateral loads

The model implemented and used in the previous chapter is a plane model based on the capacity of a cable system to carry vertical loads. Cable systems, when treated as linear elements are characterized by zero stiffness out of their plane: any combination of cable forces have its resultant in the cable plane. Therefore in design for lateral loads of cable-stayed systems, the spatial arrangement of cables with respect to the girder and the towers is very important.

Flexibility under lateral loads depends on different structural schemes adopted. In general the contribution to lateral resistance and stability comes from a combination of the following capacity of the structural elements:

1. lateral bending stiffness of the girder
2. lateral stiffness of the towers
3. assembly of the cable systems

Bridges with single-plane or parallel-plane cables systems can resist lateral loads in two different ways [10]. The first can be described as a pendulum effect; it is a second order effect based on the capacity of the system to store potential energy that can counteract the lateral excitation. This mechanism, which is effective only

in earth-anchored system, gives stability to the system for lateral loads even when the lateral resistance of the girder is negligible. The second behavior is typical of self anchored systems in which the girder resists lateral forces through bending; as a consequence, the motion due to lateral loads consists mostly of a rotation of the girder around the ideal vertical axis of tower, instead of a rotation of the girder around the ideal point at the top of the tower.

A different behavior in terms of lateral stiffness comes from a "spatial" arrangement of the cable system, in particular a truss effect can be obtained moving the cable systems to two or more different planes and taking into account the contribution to lateral stability of the resultant force due to the tension of at least one of the cable systems, the other being in compression. The compressed system, to remain stable must be designed in such a way that compression in the cables under live loads does not exceed the level of tension related to initial stresses due to dead loads.

Of course the behavior or real systems consists of a mixture of the different patterns briefly illustrated above. In the following section I will investigate some of the issues related to cable-stayed bridges behavior under lateral loads, with particular attention to dynamic effects.

3.2 Description of the model

In the first part of my thesis I have constructed a simple model of a cable-stayed bridge to perform a static analysis: the purpose was to test the model for further more advanced analyses. I have considered a plane model structure neglecting the out-of-plane effects, such as torsional effects and lateral bending; furthermore, I have only considered symmetrical load conditions, without including second order effects. The towers have been modeled as compression columns neglecting the effect of bending on the compressive stiffness, the girder itself has been modeled as a beam, in which bending and compression, do not interact in the definition of the stiffness matrix. As a consequence, I have not adopted the beam-column model, for the tower as for the girder, which is needed to check for the instability of the system.

3.2.1 Characteristics of the structural elements

In the following analysis both the tower and the deck are composed of steel elements. The material is linear elastic, Young modulus is $E = 2.05x10^5 MPa$, material density is 7.85 KN/m^3. The same density has been considered for the steel cables; however, the Young modulus was reduced to $E = 1.9x10^5 MPa$, as it is usually done to take into account the effect of the wires assembly in the cables [16]. The steel for the tower and the deck is a grade 50 steel (ultimate strength $\sigma_{ult} = 350MPa$), while the cables' material is an high-strength steel with an ultimate strength of $\sigma_{ult} = 1,600MPa$.

The geometric data are those derived through the plane simplified model, the lower inertia scheme is adopted for the girder. To expand the model out of the original plane, an hypothetical box section is adopted; the box section is $18m$ wide and $1.5m$ deep. The steel girder has constant area of $A = 1.307m^2$ and a longitudinal inertia of $I_{long} = 0.54m^4$, a lateral inertia of $I_{lat} = 38m^4$, and a total torsional moment of inertia $I_{tor} = 1.908m^4$. The total area of the tower is $A^t = 1.2m^2$ and its longitudinal total inertia is $I_l^t = 4.5m^4$. It results in a H-shaped structure, composed of hollow section beam elements, two vertical and two transverse elements, each one has constant area of $A^{ti} = 0.6m^2$ and a longitudinal and lateral inertia of $I^t_{lat,long} = 2.25m^4$

These characteristics have been derived from the analysis developed with the plane model of the structure. The cables have been dimensioned on the basis of an uniform distribution of the dead load of $g = 100KN/m$ along the deck, a pretension is applied to four of the central cables on both side of midspan point to accomplish the requirement of uniform vertical stiffness. The maximum value of the strain in the cables is 0.337%. In Table 3.1 the main characteristics of cables' system are presented. Cables areas indicated refer to the single cable. Although in Table 3.1 they are only numbered from 1 to 18, (they correspond to the flanking span), they form two parallel planes on both sides of the pylons. However, cables on both sides of the central span have the same characteristics of these cables that are their symmetrical with respect to the tower.

A pseudo-linear analysis can be developed estimating a modified value of the

Table 3.1: Geometric Characteristics of Cables - $I_{girder} = 0.54m^4$

	$A_{cab}(cm^2)$	ϵ	σ/σ_u	$E_{red}(MPa)$	$F_{pres}(KN)$
1	18.44	0.337%	40.0%	1.899e+05	0
2	12.96	0.337%	40.0%	1.899e+05	0
3	13.86	0.337%	40.0%	1.897e+05	0
4	14.65	0.338%	40.0%	1.896e+05	0
5	15.77	0.338%	40.0%	1.894e+05	0
6	16.99	0.338%	40.0%	1.892e+05	0
7	17.79	0.339%	40.0%	1.890e+05	0
8	19.09	0.339%	40.0%	1.887e+05	0
9	22.35	0.311%	36.6%	1.879e+05	0
10	25.92	0.280%	32.6%	1.865e+05	0
11	31.68	0.247%	28.4%	1.838e+05	0
12	38.90	0.219%	24.5%	1.790e+05	0
13	44.89	0.202%	21.7%	1.724e+05	0
14	58.39	0.181%	17.6%	1.558e+05	0
15	82.32	0.177%	14.3%	1.291e+05	289
16	89.78	0.184%	14.9%	1.291e+05	747
17	103.46	0.191%	15.4%	1.291e+05	1,420
18	177.91	0.198%	16.0%	1.291e+05	3,310

Young modulus expressed as a function of the cable length and the level of tension according to equation (2.15) known as the Ernst formula [7], which can be used in a step by step analysis updating the value of tension at each step.

As can be seen from Table 3.1, though the reduced modulus is superior to 95% of the original Young modulus for the first eleven cables starting from the tower, the decay greatly increases starting from the twelfth cable.The values of the pre-stressing forces calculates as shown in Chapter 2 are here indicated in the sixth column of Table 3.1. Equation (2.15) shows a trade off between the area of cable and the Young modulus for constant value of tension; as a consequence, the initial tension must be tuned up in order to keep the initial stiffness constant on the cables. Of course the reduced modulus is very low and reaches the minimum value at the midspan cable (35.7 % of the original Young Modulus).

For long spans the assumption of linear behavior of the cables, with constant Young modulus reduced to the initial value, can be too conservative for symmetrical

loading. In fact the effect of this kind of loading is an increase of tension in all the cables, the increase in tension bring to an increase in stiffness, that it is not considered if the elastic modulus is not updated.

A similar geometric non-linear effect comes from the beam-column model: in particular it is a reduction of the bending stiffness related to the compression on the elements; in my model both the tower and the deck experience high level of compression stresses and this effect tends to be relevant. In contrast with the increase in stiffness experienced by the cables, in the beam and the tower there is a trade off between tension and stiffness. As I pointed out above, a cable-stayed bridge is a complex structure, its behavior is governed by the interaction of different kind of structural members, in order to study the real deformation of the structure it is necessary to model all the non-linearity of the system.

3.2.2 The finite element model

I have discussed the process of transforming a physical model into a mathematical model for my bridge structure. The following step is to define how to solve this model: this has been done with a finite element model. The finite elements that I have implemented in my model to perform my analysis are part of the ADINA [4] library and are the following:

1. Truss 2-node element for the cables. This element can be successfully adopted to describe elements with no bending and shear resistance, in the case in which the applied forces are only end forces. The element in ADINA can be employed in linear, materially-nonlinear-only and large displacements and rotation but with small strains. The same element varies in a 3-node and 4-node truss element.

2. Two nodes beam elements for the tower and the deck. The beam element is the 2-node Hermitian beam, which is based on the Bernoulli-Euler beam theory. It is corrected for shear deformation effects and can be employed in linear, materially-nonlinear-only and large displacements and rotation but with small strains, both in elastic and elasto-plastic analysis.

3.3 Linear elastic analysis

I have performed the first analysis on a simple linear elastic model; all the calculation were referred to the undeformed geometry, the cable sag has not been considered and the weight of the cables was neglected.

The starting status of the system includes all the initial values of strain in the cables, and the pre-stressing forces where needed. A 2-node truss element with a straight line axis has been adopted to describe the behavior of cables in a linear analysis. The deck has been modeled with a finite element mesh that divided each beam between two adjacent cables in three parts 5 m long, the beam was modeled by 2-node Hermitian elements. In particular, the model adopted is a spine model: the box section is not modeled with plane elements but only with simple beams, that include all the characteristics of the box section; the connections between the girder beam and the cables is modeled with transverse beams (2-node Hermitian elements) with high level of stiffness characteristics, they have just to rigidly connect the main girder to the cables and the towers, without introducing any flexibility into the model. For a scheme of the structure see Figure 3-1.

Similarly to the main girder, the tower has been modeled with 2-node Hermitian elements, each element being 5 m long. The elastic modulus of the cables has been considered constant and equal to the initial value calculated using equation (2.15), after the pretension of the cables, the stiffness has not been updated when the tension in the cables changes after the application of the live load. In the same way the stiffness of the other elements has been considered constant for all the load conditions, the analysis of the system has always been performed without considering the effect of the deformation on the loads, the integration of all the variables has been done with respect of the initial geometry of the system, and the stiffness matrix formed by terms which are constant with the external load.

The system is simply described by general equation of motion, formulated as following; solving the equation (3.1), the displacements u will be found. For a generic

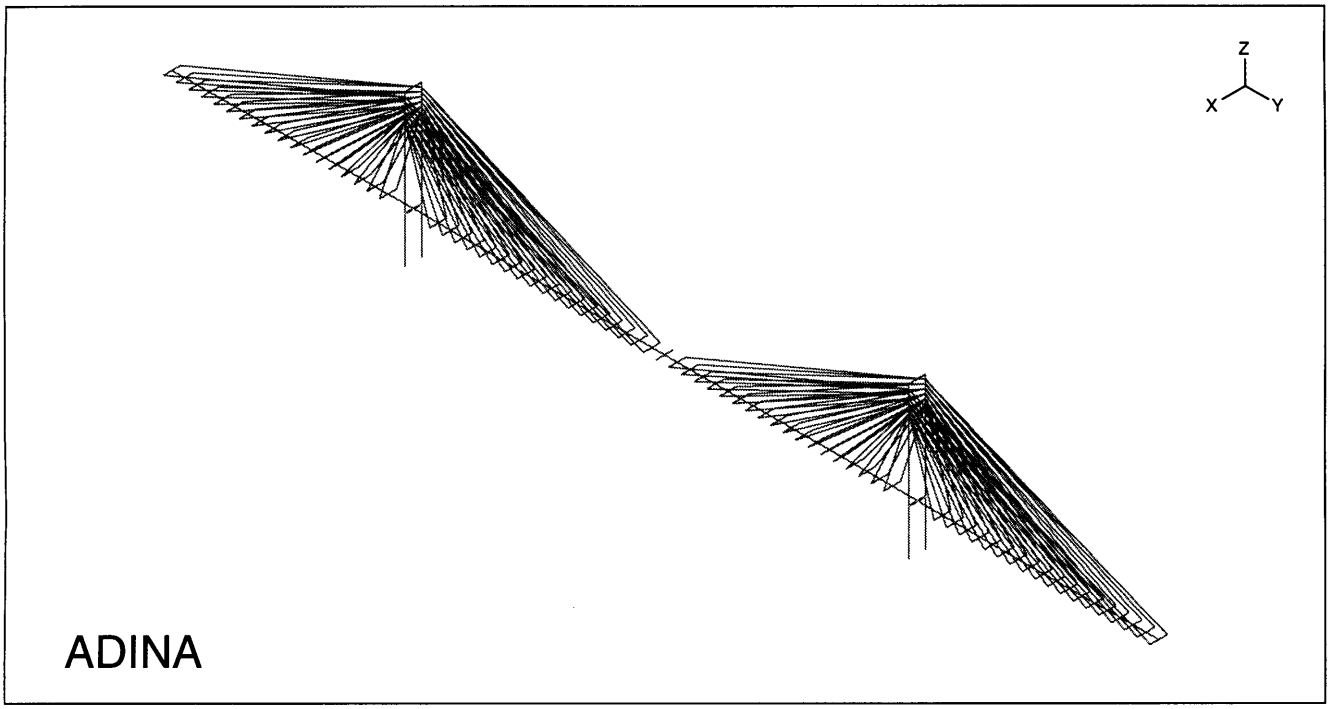

Figure 3-1: Three dimensional model

load condition represented by $R(t)$, this is the form of the equation:

$$[M][\ddot{U}] + [C][\dot{U}] + [K][U] = [R] \tag{3.1}$$

The mass matrix is defined assuming lumped-masses throughout the system.Damping can be assumed as proportional to K and M in the following Rayleigh matrix format:

$$[C] = \alpha_1[M] + \alpha_2[K] \tag{3.2}$$

The same model has been used for a linear dynamic analysis, for a first check on the first fundamental periods of the system and for the analysis of the main vibration modes.

3.3.1 Modal analysis results

The first analysis of the space structure is made through modal analysis. In particular, the equations of motions expressed in matrix from 3.1 are rewritten after the basis of vector U is changed through the following position.

$$U(t) = \sum_{j=1}^{n} \phi_j q_j(t) = \phi_j q(t) \tag{3.3}$$

In particular this form help in finding uncoupled equations of motion then reducing, a Multi Degree of Freedom system in the summation of a series of SDOF system. The characteristics of each SDOF system are found with the solution of the following eigenvalue problem for the undamped system:

$$[K][\Phi_j] = \omega_j^2[M][\Phi_j] \tag{3.4}$$

The eigenvectors of the problem are those that satisfy equation 3.4 together with the orthogonality relations:

$$[\Phi_i]^T[K][\Phi_j] = \omega_j^2[\Phi_i]^T[M][\Phi_j]\delta_{ij} \tag{3.5}$$

where δ_{ij} is the Dirac function, which is zero when i is different from j and unity when they are the same. The characteristics of the equivalent SDOF's are given by the following modal mass, modal stiffness, and modal damping.

$$\tilde{M}_j = [\Phi_j]^T[M][\Phi_j] \tag{3.6}$$

$$\tilde{K}_j = [\Phi_j]^T[K][\Phi_j] = \omega_j^2 \tilde{M}_j \tag{3.7}$$

$$\tilde{C}_j = [\Phi_j]^T[C][\Phi_j] \tag{3.8}$$

Assuming a linear damping, for example $[C] = \alpha[K]$ it follows that:

$$\tilde{C}_j = \alpha \tilde{K}_j = \alpha\omega^2 \tilde{M}_j \tag{3.9}$$

All of the above leads to the following n uncoupled equations for the MDOF system:

$$\tilde{M}\ddot{q}_j + \tilde{C}\dot{q} + \tilde{K}q = \phi_j R(t) \tag{3.10}$$

The values of the periods calculated through an ADINA simulation, with damping neglected, are reported in Table 3.2, together with the maximum value for the eigenvectors. For the first eight eigenvectors in the Table is also reported the direction of the mode, where V stands for vertical, L for lateral and T for torsional. A better understanding of the correspondence between modal frequencies and mode shapes comes from the mode shapes given in Figure 3-2 and in Figure 3-3. The eigenvectors that results from the output of the program are normalized; therefore, the modal mass is a unity mass and the modal stiffness is equal to the natural frequency squared. As a consequence of that, the uncoupled equations of motion, for linear damping will have the following form:

$$\ddot{q}_j + \alpha\omega_j^2 \dot{q} + \omega_j q = \phi_j R(t) \tag{3.11}$$

Table 3.2: Periods and maximum eigenvectors for each mode

MODE	PERIOD	X-EIGENVEC.	Y-EIGENVEC.	Z-EIGENVEC.	
1	7.768	4.07501e-04	-1.74936e-05	-4.60653e-05	L
2	5.137	-2.92237e-05	-1.20942e-04	-4.39015e-04	V
3	4.476	3.91150e-05	1.16609e-04	-3.72863e-04	V
4	3.401	5.93797e-04	-2.33129e-05	-4.97727e-05	L
5	3.159	4.19404e-05	-7.39451e-05	-5.21677e-04	L
6	2.872	-7.41358e-04	-4.33993e-05	1.85985e-04	V
7	2.690	3.06171e-04	-9.39401e-05	-4.22521e-04	V
8	2.580	8.46607e-05	5.03072e-05	4.11243e-04	T
9	2.578	6.45454e-05	2.17524e-05	3.78273e-04	
10	2.351	4.19838e-04	3.68961e-05	-3.04328e-04	
11	2.022	-3.93350e-04	-3.91421e-05	3.16857e-04	
12	1.899	3.87730e-05	3.88964e-05	-3.88984e-04	
13	1.877	5.04349e-05	-3.77399e-05	-3.84676e-04	
14	1.727	-5.21152e-05	3.07086e-05	3.89500e-04	
15	1.651	2.96227e-05	2.38013e-05	-3.22123e-04	

Legend: L=Lateral Mode, V=Vertical Mode, T=Torsional Mode

3.4 Non-linear formulation

I have already pointed out why the analysis of large cable stayed bridges requires a non linear analysis, this is particularly important if the serviceability requirements on the displacements, velocities and accelerations are a concern. A non linear static and dynamic finite element analysis is most effectively performed using an incremental formulation, in which the static and kinematic variables are updated incrementally corresponding to successive load step or time steps in dynamics.

In this section I report the basic of a non-linear model that I have tested in other applications on the same model of a cable-stayed bridge. Although I do not report here any particular results, I outline the basic criteria used for that model, as a starting point for new more refined analyses.

The analysis constraints are very important for this formulation [1]. On the one hand it is important that the governing finite element equations are satisfied in each load step or time step with a sufficient accuracy because otherwise solution errors can accumulate; this requires small load increments or time steps. On the other hand if these steps are too small the analysis can become too expensive. The attention must focus on the right choice for the iterative solution method, for the tolerance of the solution, for the limit in the iteration and especially for load increments or time steps.

The expression of the governing equations for the response of the finite element system in static analysis is

$$^{(t)}[K][U] = ^{(t+\Delta t)}[R] - ^{(t)}[F] \tag{3.12}$$

where $^{t}[K]$ is the tangent stiffness matrix corresponding to the configuration of the system at the time t, $[U]$ is the vector of nodal point of incremental displacements, while $[R]$ is the external force calculated after the increment of time and $[F]$ is calculated at time t.

Similar to equation 3.12 the following expression describes the finite element equations of motion in which the internal force given by the product of the mass$[M]$ and

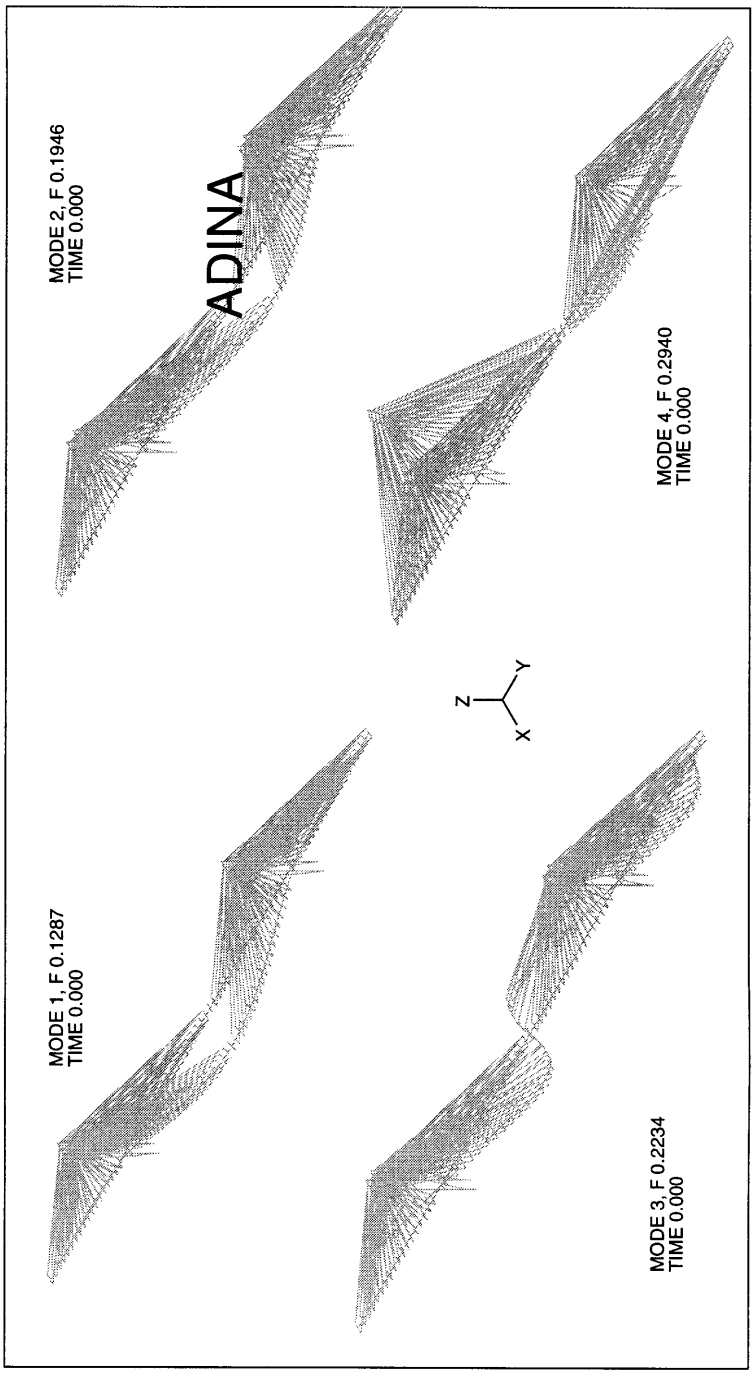

Figure 3-2: Modes 1^{st} to 4^{th}

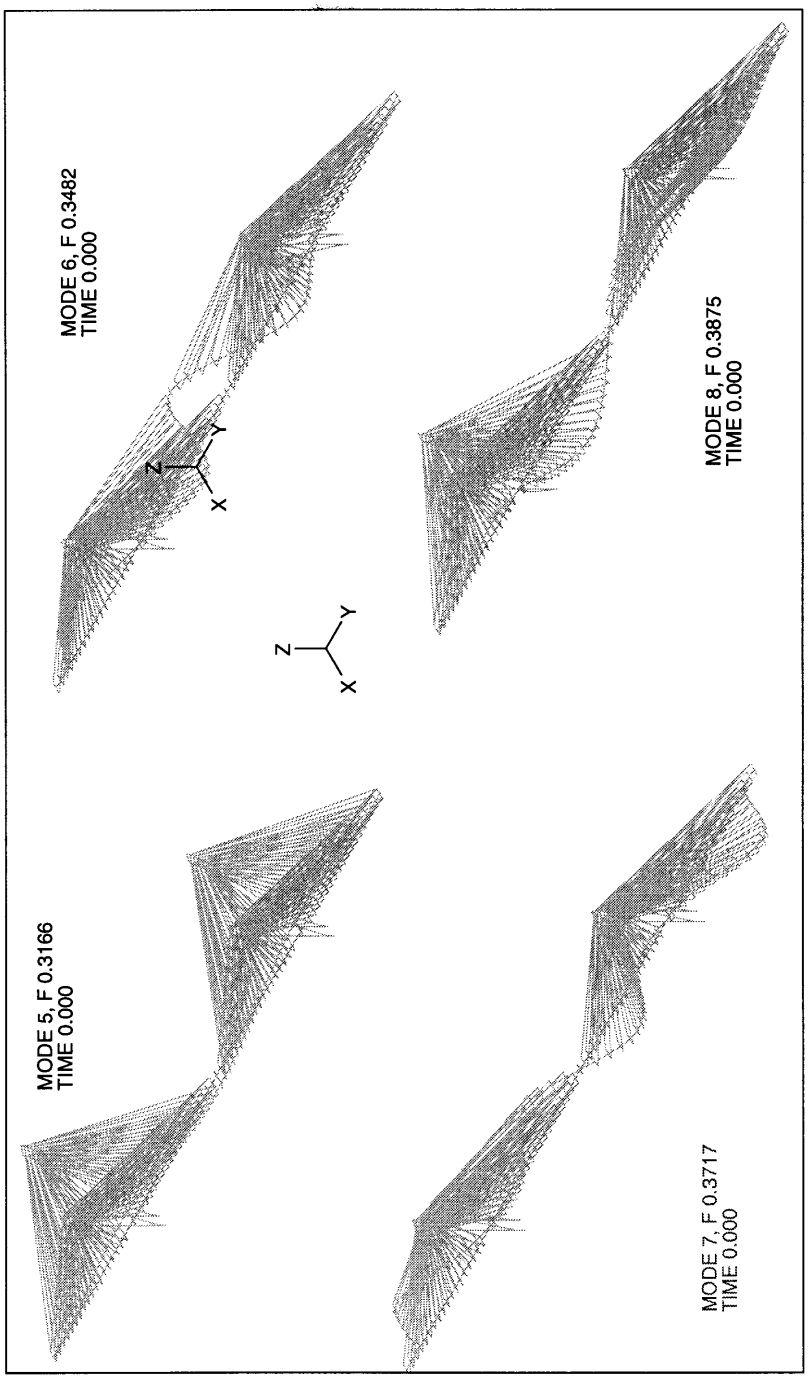

Figure 3-3: Modes 5^{th} to 8^{th}

the acceleration after the increment of time is included

$$^{(t)}[K][U] =^{(t+\Delta t)} [R] -^{(t)} [F] -^{(t+\Delta t)} [\ddot{U}] \tag{3.13}$$

In my problem this formulation has been applied to take into account the large displacements analysis, implemented to better describe the behavior of the cables when they deform under the effect of their weight; furthermore, the geometric nonlinear behavior of the tower and the deck was considered by updating at each load increment or time step the stiffness matrix. In this formulation the tangent stiffness matrix gives an exact description of the system in its stress-strain status corresponding to the actual value of the loading; the hypothesis of small strains was still valid.

The finite elements adopted to describe the system are the 2-node truss element for the cables and the 2-node beam element for the tower and the deck. The only difference is that each cable is described by a mesh of more than one element, the number of elements varies with the length of the cable in such a way that the maximum length of each element does not exceed 15 m. This must be done in order to describe the cable sag under the effect of the weight; an initial strain due to the pretension of the cable has been applied on the initial configuration. This evaluation has been based on the reduced modulus of the cable calculated from equation 2.15

The solution of the system was obtained through the Broyden-Fletcher-Goldfarb-Shanno (BFGS) matrix update method, with the use of line searching method, the line searching tolerance (STOL) was set to 0.5. The tolerance criterion for the convergence of the iteration was the force criterion with an assumed tolerance of 10^{-5}.

Chapter 4

Modeling of wind actions

In this chapter I review the fundamental phenomena related to wind actions on bridge structures. Different wind effects and interactions between wind forces and bridge structures can yield to strong motion of bridge decks, cables and towers and have to be taken into account in designing both for strength and for serviceability. The basic means of limiting these effects are introduced also with particular care for the construction phase of long span bridges.

The steady-state part of the wind excitation can be addressed through an approximate static analysis. Apart from that, many different phenomena related to win actions can bring dynamics effects to bridge structures. These actions, which are particularly relevant for long span flexible bridges such as suspension and cable-stayed bridges, can also be related to low speed actions. Analog testings of model structures in wind galleries have shown that for these bridges wind-structure interaction phenomena are highly related to the cross section shape of the girder. For example, it has been observed [23] that plate stiffened deck systems are often exposed to excessive vortex shedding excitations for transverse wind actions. As a consequence of that, the deck experiences excitations in vertical bending. The problem can be solved through a reshaping of the cross-section; in fact, the design of edge details can be fundamental in these cases. Box sections or concrete decks with box edge girders, which are commonly used in a large number of existing cable-stayed bridges, have shown a good aerodynamic response to wind actions.

The chapter is organized as follows: I will first introduce the basic laws for distribution of wind forces, secondly I will discuss the static and dynamic components of wind actions. This will be more an overall description of the phenomena and will not include a complete analytical formulation of the problem. Therefore, the conclusion of this brief description is that wind-structure interactions phenomena are addressed through different types of models. The different analysis aspects are not unified under the same theory and the action analysis requires models that do not coincide with those usually applied to structural analysis. A strong effort is still needed towards the unification of all the theories under the same simulation model, and, even though the growth of Computational Fluid Dynamics is quite fast, analog testing is still the most valuable resource used in practical applications.

4.1 Wind action description

Wind is slowed down near the earth's surface by the resistance to the flow introduced by the roughness of the ground and by fluid friction associated to the air viscosity. As a result, the wind velocity varies from zero at the surface to the gradient wind at about 300 m to 600 m above the ground surface. In a typical distribution of wind force as a function of the height z the mean wind speed,V is described by a power law such as:

$$\frac{V(z)}{V(z_0)} = (\frac{z}{z_0})^{\alpha} \tag{4.1}$$

where the exponent α is in the range from 0.12 to 0.5 and directly increases with the terrain roughness; z_0 is a reference height.

The shearing action of the wind also causes mechanical turbulence of the flow, known as gustiness; its effects are continuous and sometimes abrupt changes in direction and magnitude of the wind. The wind turbulence is characterized by a random distribution of the physical size of the disturbances, this is in the range from almost zero to several hundred meters in length, while the disturbances in the lateral

direction are less extended.

Gust distribution is very similar to the mean velocity distribution, and can be described by the following [10]

$$\frac{V_{gu}(z)}{V_{gu}(z_0)} = C_{gu}(\frac{z}{z_0})^{0.1} \tag{4.2}$$

in which C_{gu} is the gust factor, that can be taken as equal to 1.41. In the following two sections I describe separately the static and the dynamic effects of wind actions on structures.

4.2 Wind actions as static loads

The first component to analyze is the static one, which represents the steady state part of the wind action. It always acts in any structure and is particularly relevant for large span structures. On a bridge cross section, the static action consists of a drag component, D, acting in the wind direction, a lift component, L, normal to the wind direction and a pitching moment, M. All these three components are governed by the wind speed, V, the air density, ρ, the cross sectional width, B, and the dimensionless coefficient, C_D, C_L and C_M. The expressions describing these actions are

$$D = \frac{1}{2}\rho V^2 B C_D \tag{4.3}$$

$$L = \frac{1}{2}\rho V^2 B C_L \tag{4.4}$$

$$M = \frac{1}{2}\rho V^2 B^2 C_M \tag{4.5}$$

where the values of the C coefficients are normally determined experimentally in wind tunnels. These coefficients are dependent on the cross-section geometry and are a function of the wind incident angle β. They are also used in the calculation of the

bridge response to turbulent wind.

All the structural parts need to be designed to bear these actions, the value of the design average wind speed can be derived from measurements, and it is usually associated to a mean recurrence interval of time that is calculated on a statistical basis. Different values of the average velocity and of the recurrence interval can be assumed for serviceability design and for limit strength design.

4.3 Dynamic effects of wind actions

The dynamic actions to take into account in the analysis of slender cable-stayed bridges are those related to vortex shedding, torsional instability and flutter, galloping, wake instability, and buffeting by turbulence. For local effects on the cables it is important to consider the joint occurrence of wind and rain. All these effects need designer's attention for their consequence on strength and serviceability not only after the completion of the structure but also during the construction phase. In fact, cable-stayed bridges are highly redundant structures but during erection are much more flexible than they are in their final configuration.

In the following paragraphs I will briefly describe the different dynamic phenomena related to wind-structure interaction. Although many of these effects are better understood by analog wind-testing on model structures, recent developments in the field of numerical models and information technology can hopefully help to achieve more reliable computer simulation models.

4.3.1 Turbulence

Wind action varies randomly with time, due to the turbulence of the air flow. This aspect is of great interest in structural engineering application as it introduces time dependent load conditions in the analysis. Structures with low natural frequencies may exhibit resonant amplification effects in their response to wind action. Furthermore, longspan structures' aerodynamic behavior strongly depend upon the turbulence in the air flow. A quantitative description of turbulence is necessary when it has to be

taken into account for design issues. The simplest descriptor of wind turbulence is turbulence intensity. It is defined with respect to the height z as:

$$I(z) = \frac{\sqrt{(v_{fl}^2)}}{V(z)} \tag{4.6}$$

where $v_{fl}(z) = v(z,t) - V(z)$ represents the velocity fluctuations with respect to the mean velocity. In order to express the turbulence intensity of an event, this must be related to a time interval. This is usually assumed between 10 minutes and one hour, and depends on the data collected.

4.3.2 Spectra used for structural design purpose

They are used to describe the frequency content of turbulent wind action. A simple formula for the spectrum definition is:

$$\frac{nS(z,n)}{v_*^2} = \frac{200f}{(1+50f)^{5/3}} \tag{4.7}$$

where n represents the frequency, v_* is the friction velocity, and is related to the mean wind velocity $V(z)$ through the following formula expression:

$$V(z) = \frac{1}{k} v_* ln \frac{z}{z_0} \tag{4.8}$$

that express the the mean wind speed at a certain height as a function of v_*, contain an explicit indication of k known as the Von Karman constant and the roughness length z_0 that depends on the different soil characteristics.

All the power spectral density functions are expressed as function of a non-dimensional frequency given by the product of the frequency by the "autocorrelation length" and divided by the velocity. These spectra characterize the wind excitation as a random signal. Figures 4-1, 4-2 and 4-3 show different power spectral density functions available in the literature.

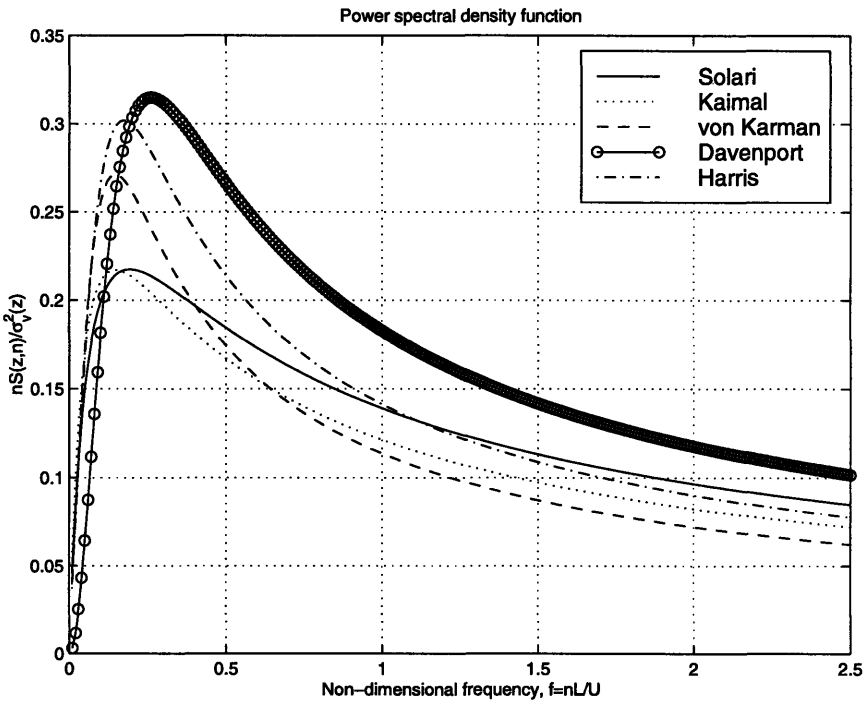

Figure 4-1: Power spectral density functions variation with non-dimensional frequencies

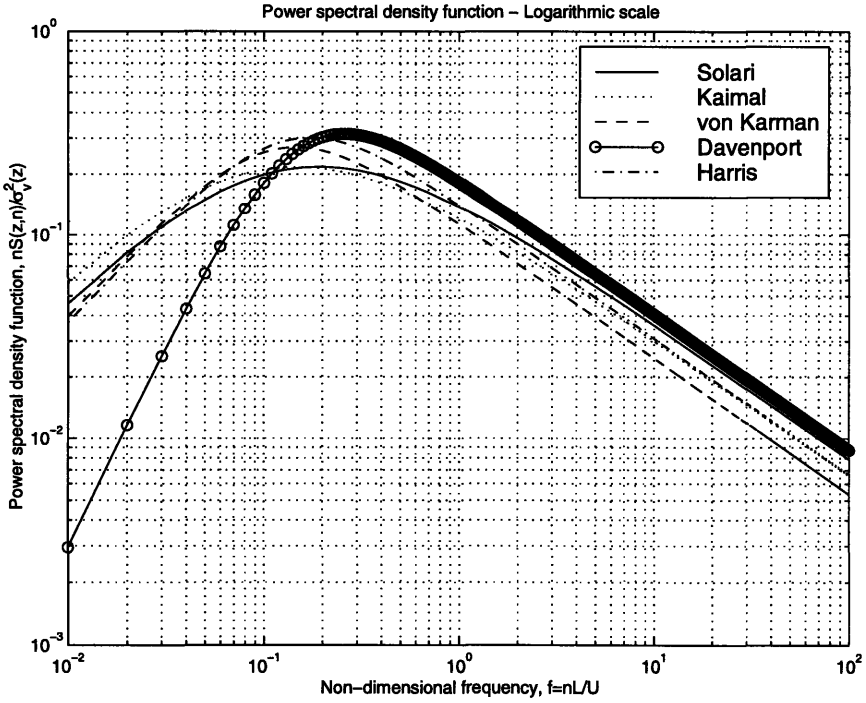

Figure 4-2: Power spectral density functions variation with non-dimensional frequencies - log scale

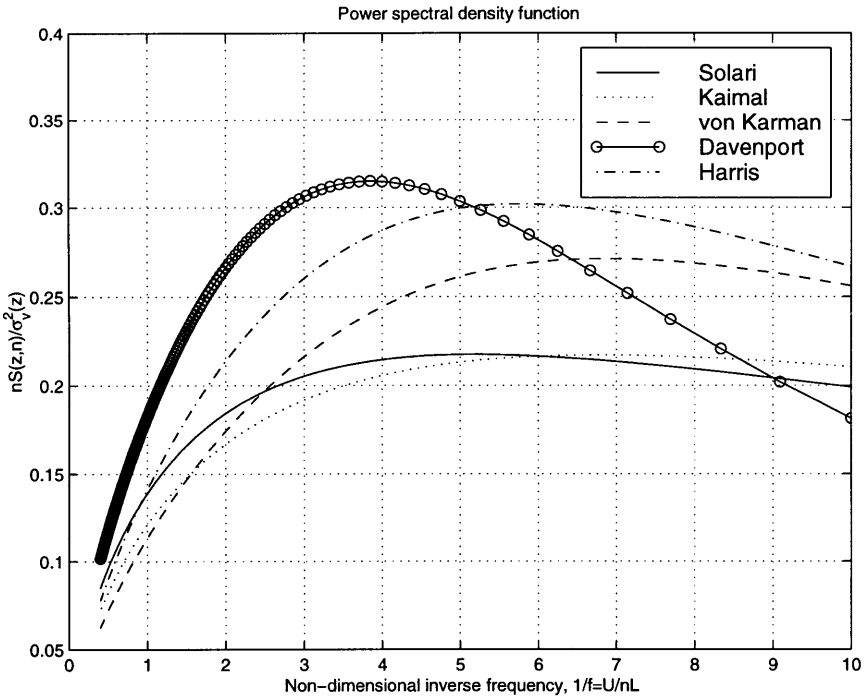

Figure 4-3: Power spectral density functions variation with non-dimensional inverse frequencies

Another expression to be used in the spectrum definition is the Monin (or similarity) coordinate f, which is:

$$f = \frac{nz}{V(z)} \tag{4.9}$$

This formulation for the wind spectra applied to the lowest frequencies overestimates (5 percent) the structural response, furthermore it does not satisfy the requirements for n=0 but in any case it applies with good results to calculation of the spectra to be used in structural analysis. In order to apply this formulation to define the wind velocity spectrum at a certain height z, v_* can be calculated from (4.8), after having defined a value for the mean velocity $V(z)$ and a proper value for the roughness length z_0.

4.3.3 Vortex shedding

The vortex shedding excitation is typical of slender cylinders exposed to wind action, this is an across-wind action and can occur even for not particularly strong wind actions. Wind forms vortices alternately in either side of the section when flowing around these elements; this phenomenon has a high degree of periodicity. Vortex shedding can occur on other kinds of bluff sections different from cylindric, typically on box type sections. The magnitude of this action greatly decays when the edges of the cross section are shaped with streamlining profile. To describe the relation between the frequency of vortex shedding, f_s, and the wind velocity, I introduce the Strouhal Number, S, defined as a coefficient that depends on the geometric shape of the section. For a cylinder of width B, it can be expressed by the following:

$$S = \frac{f_s B}{V} \tag{4.10}$$

For circular cylinders this number depends on the Reynolds Number, $Re = VB/\nu$, where ν is the kinematic viscosity of air. In the case of sharp cornered cross sections the Strouhal Number is independent from the Reynolds Number.

When the vortex shedding frequency, f_s, is closer to the deck natural frequency for torsion or vertical bending, bridge vibrations can develop. This happens when the wind velocity is very close to the critical speed, which is a characteristic of the structure. In this case the amplitude will strongly depend on the structural damping of the whole structure. The value of critical wind speeds, for long span bridge structures are in the narrow range of 8 to 15 m/sec, these values are not related to extraordinary events. However, vibrations of bridge decks related to vortex shedding are mostly vertical and the maximum amplitudes are not as larger as in other more slender cantilever structures. Design for vortex shedding tends to limit the amplitude of oscillations more for serviceability concerns than for stability. The acceptable acceleration threshold for users' comfort is 2 percent of gravity acceleration g, for wind speeds below 15 m/sec, and a maximum of 5 percent of gravity acceleration, for wind speeds between 15 m/sec and 30 m/sec.

Vortex shedding excitation of circular cylinders is sensitive to the mass damping parameter, defined as $\zeta m/\rho B^2$, where m is the unit mass distributed over the length, and ζ is the critical damping ratio. It is proved that when the value of this index is equal or greater than 5 no motion will occur. A solid steel rod would have a value of this damping parameters close to 5 when a value of critical damping ratio of 0.1 percent is assumed. Stay cables in synthetic sleeves with cement grout have lower values of $\zeta m/\rho B^2$ and can experience vortex shedding excitations: the consequences will be undesired local effects of bending at the cable anchorage, with high stress concentrations, and cable induced vibrations on the deck and the tower. Some very simple viscoelastic collars at the cable attachments can highly increase the structural damping and prevent the cables from this undesired behavior.

4.3.4 Torsional instability and flutter

Although torsional instability and flutter are both related to the twisting of the bridge deck around its longitudinal axis, it is important to separate the two problems. The basic difference is that torsional instability derives from a single degree of freedom motion whereas flutter results from the coupled effect of torsional and flexural motion. Both of these wind-structure interaction effects are unstable and can easily drive long span bridge structures beyond their limit strength and to collapse.

Torsional instability by itself comes from the second order effect related to the twisting moment expressed by (4.5). As the twisting moment increases with the wind velocity, the effective angle of attack of the wind relative to the structure may increase too. This leads to a further increase of the twisting moment, that will require an additional reactive moment from the structure. This is clearly a non-linear instability phenomenon, related to the inertia characteristics of the structures, to the wind velocity, to the shape of the section and to the angle of attack of the wind action.

Critical wind velocity for torsional instability corresponds to the value of wind velocity at which the magnitude of the wind induced moment creates an unstable condition on the structure. This effect can cause the structure to collapse if the ultimate strength is reached. In a simple model of a deck with a concentrated torsional

spring of elastic constant , if is the angle of rotation of the section of width B, the critical wind velocity for the moment expressed by (4.5) is given by:

$$U_c = \sqrt{\frac{2K_\theta}{\rho B^2 C'_M}} \tag{4.11}$$

where:

$$C'_M = \frac{dC'_M}{d\theta}|_{\theta=0} \tag{4.12}$$

Uc is also called critical divergence velocity, and normally, even for large span structures is well above the value of critical velocity for vortex shedding.

Torsional instability is not sensitive to structural damping. The critical divergence velocity increases with torsional rigidity as it is shown in (4.11). As torsional rigidity is directly related to natural frequencies, it follows that the objective of the design for torsional instability is to realize bridge decks where the torsional modes are high frequency modes. The critical divergence velocity is also inversely correlated to the width of the deck, thus, narrow decks are less sensitive to torsional instability.

As stated above, flutter is basically related to the coupling of torsional and bending modes in the motion due to dynamic excitation. An essential part of the instability in these oscillations is based on the phase difference between the torsional and the bending motion. The critical wind speed that causes the instability has to be evaluated, the design wind speed, then, must be well above this critical value. This design objective is a priority in long span bridges, in fact, the amplitude of motion caused by flutter can reach catastrophic values for long span decks.

Bridges with high values of natural frequency are less sensitive to flutter, as a consequence, torsional stiffness must be a concern for long span structures; in cable-stayed bridges for example the contribution of the tower shape is relevant to the overall torsional response to dynamic wind action. Similarly, cable disposition is important for deck torsional rigidity, for longer spans; for example; the disposition of the cables on a single plane at the center of the cross section will require a very high torsional

stiffness of the deck. The critical wind speed for flutter is also dependent on the ratio of torsional natural frequency to bending natural frequency, f_θ/f_y; the bridge decks are susceptible to flutter if this ratio is only slightly higher than unity. If the ratio is higher than 1.5 flutter would not occur. The fundamental dynamic equations in two-dimensional form can be written as follows [20]:

$$m(\ddot{y} + 2\zeta_y\omega_y\dot{y} + {\omega_y}^2 y) = L \tag{4.13}$$

$$I(\ddot{\theta} + 2\zeta_\theta\omega_\theta\dot{\theta} + {\omega_\theta}^2\theta) = M \tag{4.14}$$

where, by definition, ω is the circular frequency, θ and the index θ stand for the rotation around the longitudinal axis, y and the index y stand for the vertical displacement. As defined in (4.4) and (4.5), L and M are the lift force and the twisting moment, so the equations (4.13) and (4.14) can be rewritten as:

$$\rho V^2 B(kH_1^* + kH_2^*\frac{B\dot{\theta}}{V} + k^2 H_3^*\theta) = L \tag{4.15}$$

$$\rho V^2 B^2(kA_1^*\frac{\dot{y}}{V} + kA_2^*\frac{B\dot{\theta}}{V} + k^2 H_3^*\theta) = M \tag{4.16}$$

where, by definition, $k = B\omega/V$.

In the above equations (4.15) and (4.16), $H_{1,2,3}^*$ and $A_{1,2,3}^*$ are the flutter coefficients; they depend on the aerodynamic properties of the section, are all functions of k, and can be derived experimentally. As mentioned above, flutter is a two degree-of-freedom phenomenon and both the lift and the moment equation are required to predict the flutter critical velocity of a long-span bridge. In this analysis the coupling coefficients, H_2^* and A_1^* become as important as A_3^*, which is a measure of aerodynamic torsional stiffness.

Torsional instability can also be described by equations (4.15) and (4.16), but, as it is a single degree of freedom phenomenon, only the moment equation (4.16)

is relevant. In this equation the coefficient A_2^* determines the degree of torsional instability. Similarly H_1^* determines the degree of stability in vertical bending, H_1^* is usually negative, except for those bridge decks that are prone to vortex shedding excitation, in which case it is positive over the wind speed range where vortex shedding excitation occurs.

The conclusion is that equations (4.15) and (4.16) fully describe the phenomena of wind structure interaction for dynamic excitation, for torsional and bending moment, and can then include both torsional instability and flutter. The response analysis for the design can be based on the H and A coefficients that are experimentally determined. It must be stressed out that these are potentially the most dangerous phenomena for cable-stayed long span bridges. In fact, they can lead the structure to instability and collapse.

Cable-stayed bridges are no less prone to these phenomena of aerodynamic excitation than suspension bridges, and this can be more relevant in the future as the limit spans are increasing rapidly. The fundamental parameter to test the sensitivity of a bridge to flutter is the ratio of torsional natural frequency to bending natural frequency. By contrast, this parameter does not have any influence on sensitivity to torsional instability.

4.3.5 Galloping and wind-rain instability

Galloping is a single-degree-of-freedom instability phenomenon that causes large amplitude motion in a cross-wind plane. It has been found that rectangular elements with width to depth ratios less than four are the most prone to galloping effects. It is important to consider galloping in the design of towers particularly during erection, before the cables and the deck are installed. The criterion for stability is related to the lift coefficient, $C_L$and the drag coefficient, C_D, and is based on the following relation [5]:

$$\frac{\delta C_L}{\delta \theta} + C_D < 0. \tag{4.17}$$

Damping is very effective in avoiding the excitation of galloping oscillations; as a result, dynamic vibration absorbers can be used to protect structural elements from this effect.

A particular effect of galloping may affect elements with cylindrical cross sections, when they are subjected to even a small change in their axi-symmetry. This can happen when water or ice films deposit on cables. On cable of cable-stayed bridges it can lead to oscillation with an amplitude of double the diameter of the cable. This can be prevented by simply connecting neighboring cables together with a wire rope.

4.3.6 Buffeting by wind turbulence

Turbulence is a fluctuation of wind speed with the time, the result is a variation of the wind load along the span of a bridge. The magnitude of the bridge response depends on the wind speed, the properties of turbulence, the shape of the road deck and the natural frequencies of the bridge.

Effects of turbulence on the bridge behavior depend on the physical scale of turbulence relative to the size of the bridge and on the effect that it has on the frequency spectrum of wind energy. Good estimates of the response can be made using analytical procedures that incorporate data from wind tunnel tests.

4.4 Conclusion and remarks

I have surveyed the wind-structure different kinds of interactions. While some of these interactions (i.e.; steady state actions) apply to every kind of structure, others, such as vortex shedding apply to bridge structure, even if they are most relevant for slender cylindrical structures. In other cases the interaction effects are strictly related to cable-stayed bridges or other long span bridges, as in the case of flutter. In some other cases the interaction regards a part of the whole system as it is for wind rain instability of cables, or finally the interaction can regard bridge structures during the construction phase, as it is for galloping for the towers before all the cables are connected to the entire deck.

In general the fundamental design aspects to be considered at the conceptual design stage are those related to the optimal cross-section shape for aerodynamic effects, together with the distribution of lateral, torsion and bending stiffness of the structure.

In fact, a good control of flow separation around the deck, together with a reduction of the surface directly exposed to lateral wind, will help achieving an optimal design for wind action. One of the objective of the design of a long-span bridge structures will be an high lateral stiffness optimized to minimize the amplitude of lateral vibrations. The contribution of the towers and of cable arrangements to lateral stability is fundamental. With respect to towers' design, A shapes show very good performances and positively contribute to lateral stability. With respect to cables' arrangements, fan patterns together with spatial arrangement on convergent planes add the cables' contribution to the overall lateral stiffness and stability of the system. I have also stressed how high torsional stiffness can improve the cable-stayed bridges overall stability, this can be controlled through the design and the shaping of the cross section of the girder.

Other design aspects are related to damping distribution along the structure. This is important in the case of modes excited by resonant components that can be contained in the wind turbulent actions. As the overall structural damping of long span cable supported structures is usually very low, in many cases it will be beneficial to think about adding damping through the application of special devices.

In some cases special devices can be used to limit wind effects during the construction phase, in fact the low lateral stiffness of the deck can bring about effects that are completely different from those that can be observed when the continuity of the girder is realized. This can suggest the application of temporarily devices such as additional stay cables or more sophisticated devices such as tuned mass dampers, which are very effective in reducing vibration amplitude related to not-impulse forces, or viscoelastic spring-dampers or friction dampers. The issue of providing additional damping to cable-stayed structure will be addressed in the following chapter. Damping is very effective in controlling vibration amplitudes of long span bridges, even if

in many cases it is not easy to evaluate as it is sensitive to frequencies.

Local vibration phenomena in the cables, especially for very long midspan cable can be annoying and can be easily avoided by simply inserting dampers in the cable-deck joint or by connecting the cables one to each other.

The lesson learned from the wind induced collapse of some long span bridges in the past, together with the experience developed during many years of wind tunnel testing, together with aeroelasticity theory and application to aero-industry, can help a lot in future development of optimal wind design of long span bridges.

In any case wind analysis of long span lightweight structures is a very complex problem that include computational difficulties both in the modeling of the flow distribution, and in the modeling of the non linear interaction between the structure and the fluid itself. In fact, the flow distribution depends on the deformed shape of the structure and vice-versa. This introduces elements of high non-linearity in the formulation and solution of the problem.

Another challenge comes from the modeling of the wind action as a random process as it is and from including the spatial effects related to the dimension of the structures.

Chapter 5

Passive devices for motion control

The long-span bridge construction and design industry is constantly moving towards two different objectives: the first is the development of new technologies that are able to address the demand for longer spans, the second is to address the increasing demand for structures whose safety and serviceability requirements are guaranteed for the whole life cycle. As a matter of fact, from an economic perspective, the two aspects are directly related. The money invested increases with the span and, as a result, the required level of performance over the entire life cycle is higher for long span bridges.

Even though in many bridges the design and construction solution is very specialized to a unique project, it is possible to identify some system solutions that can be applied throughout a large spectrum of projects. This is the case of motion control devices and systems that are becoming more important in the construction of long span bridges.

Once the model of the structure is properly defined and the acting loads too, it is possible to figure out how to control the motion of the system by designing its internal characteristics. Motion control devices and systems, which are part of the whole system, can be divided in the two broad categories of passive motion control devices and active motion control devices. In both cases the devices or systems aim to control the system response to external load, the requirements to be obtained will be based on the overall performance of the system. The difference in the definition

relates to the way the system operates; while an active system is operated through an external power supply, a passive system or device will not need any external power to be operated but will be started by the motion of the primary system itself.

In this chapter I will present a passive system, the Tuned Mass Damper (TMD), which is a simple device consisting of a mass, connected to the primary system through a spring and a damper. It is effective in reducing the dynamic response of the structure. Part of the energy of the system coming from the external excitation is dissipated by the damper inertia force.

In the last chapter I will introduce an active system for control of aerodynamic excitation, called Active Flutter Control System (AFCS).

5.1 The behavior of Tuned Mass Damper

Usual ranges of natural frequencies can show sensitiveness to both wind excitations (lower frequencies modes) and seismic vibrations (higher frequencies modes). Although a thorough analysis is required for earthquake actions, in the case of long span bridges the modes that can bring higher levels of energy into the system are more in the range of sensitivity to wind excitations. In particular, structures with natural periods of around five to eight seconds are likely to be resonant to gust excitations. In fact, winds' turbulent components have higher intensity in this range of periods.

These excitations are better controlled through damping, with the main objective of reducing the peak amplification in the response of the system. Empirical and identification studies show that medium to longspan cable-stayed systems have low structural damping for the range of vibrations that they can usually experience. It seems also difficult to introduce additional structural damping to such large structures. Therefore, one of the most interesting application comes from the use of Tuned Mass Dampers (TMD). This system has been largely and successfully applied to high rise building to control wind driven oscillations. In the following paragraphs, I will first investigate the basics of TMD theory, then I will show the basics of a design

methodology and finally I will apply it to my model derived from the simplified theory [3]. Some results, which I have obtained testing the proposed method on my finite element model, will show how powerful these devices could be when applied to long span cable-stayed systems. My simulations are limited to the use of TMD to improve the structural performances under wind actions.

5.2 Tuned Mass Damper theory for SDOF systems

The fundamental equations are derived for a SDOF system [5] and then extended to applications to MDOF systems. The basic formulation is derived for an undamped SDOF system, recalled as the primary system, to which a mass is connected with a spring and a concentrated damper. The latter will be identified as the TMD of the whole system. The mass of the damper, expressed as a percentage of the mass of the principal system, provides additional damping to the whole system through its relative displacement with respect to the primary system.

In the general case of primary systems subject to ground motion and harmonic excitation respectively expressed as:

$$a_g = \hat{a}_g e^{i\Omega t} \tag{5.1}$$

$$p = \hat{p} e^{i\Omega t} \tag{5.2}$$

The response in term of displacement has a similar form. The d index indicate damper's characteristics:

$$u = \hat{u} e^{i\Omega t} \tag{5.3}$$

$$u_d = \hat{u}_d e^{i\Omega t} \tag{5.4}$$

5.2.1 Undamped primary systems

In particular, I focus on a SDOF system of mass m and frequency ω with no damping and with a TMD of mass m_d attached to the primary system by a spring and a dashpot; the frequency of the TMD is ω_d. The fundamental properties of the composed system are the following: the ratio of the excitation frequency Ω to the natural frequency of the primary system, the ratio of the damper frequency to the natural frequency of the primary system and the ratio of the mass of the damper to the mass of the primary system. They are defined as follows:

$$\rho = \frac{\Omega}{\omega} \tag{5.5}$$

$$f = \frac{\omega_d}{\omega} \tag{5.6}$$

$$\mu = \frac{m_d}{m} \tag{5.7}$$

the responses of the primary system and of the damper have the following complex form:

$$\hat{u} = \frac{\hat{p}}{k} H_1 e^{i\delta_1} - \frac{\hat{a}_g m}{k} H_2 e^{i\delta_2} \tag{5.8}$$

$$\hat{u}_d = \frac{\hat{p}}{k} H_3 e^{-i\delta_3} - \frac{\hat{a}_g m}{k} H_4 e^{i\delta_3} \tag{5.9}$$

where the H_i factors determine the amplification of the pseudo-static responses, δ are the phase angles between the response and the excitation.

Following are the amplification factors expressions:

$$H_1 = \frac{\sqrt{\left[f^2 - \rho^2\right]^2 + \left[2\xi_d \rho f\right]^2}}{|D_2|} \tag{5.10}$$

$$H_2 = \frac{\sqrt{[(1+\mu)f^2 - \rho^2]^2 + [2\xi_d \rho f(1+mu)]^2}}{|D_2|} \tag{5.11}$$

$$H_3 = \frac{\rho^2}{|D_2|} \tag{5.12}$$

$$H_4 = \frac{1}{|D_2|} \tag{5.13}$$

where

$$|D_2| = \sqrt{([1-\rho^2][f^2-\rho^2] - \mu\rho^2 f^2)^2 + (2\xi_d \rho f[1-\rho^2(1+\mu)])^2} \tag{5.14}$$

For optimal behavior a TMD has to minimize the maximum amplitude of the primary system. This condition is obtained for a particular couple of values ρ_1 and ρ_2 solutions of the following equation:

$$\rho^4 - [(1+\mu)f^2 + \frac{1+0.5\mu}{1+\mu}]\rho^2 + f^2 = 0 \tag{5.15}$$

using the two positive roots the amplification factor H_2 will have the form:

$$H_2|_{P,Q} = \frac{1+\mu}{|1-\rho_{1,2}^2(1+\mu)|} \tag{5.16}$$

the condition for optimal behavior will be the following constraint on the roots:

$$|1-\rho_1^2(1+\mu)| = |1-\rho_2^2(1+\mu)| \tag{5.17}$$

The relation between the optimal tuning frequency and the mass ratio will be derived by substituting for ρ_1 and ρ_2 using (5.15):

$$f_{opt} = \frac{\sqrt{1-0.5\mu}}{1+\mu} \tag{5.18}$$

and will be used to express the value of the optional frequencies of the damper as follows

$$\omega_d|_{opt} = f_{opt}\omega \tag{5.19}$$

As a consequence, the following will be the expressions for the roots for equation 5.15 and for the amplification factor:

$$\rho_{1,2}|_{opt} = \sqrt{\frac{1 \pm \sqrt{0.5\mu}}{1+\mu}} \tag{5.20}$$

$$H_2|_{opt} = \frac{1+\mu}{\sqrt{0.5\mu}} \tag{5.21}$$

The expression for the optimal damping at the optimal tuning frequency is

$$\xi_d|_{opt} = \sqrt{\frac{\mu(3 \pm \sqrt{0.5\mu})}{8(1+\mu)(1-0.5\mu)}} \tag{5.22}$$

The application of a TMD to an undamped primary system add the damping that the system by itself does not have. By analogy with damped SDOF systems an equivalent damping ratio ξ_e is defined as one half of the inverse of the amplification function. In fact, from the typical expression for a SDOF with low damping ratio:

$$H = \frac{1}{2\xi\sqrt{1-\xi^2}} \simeq \frac{1}{2\xi} \tag{5.23}$$

and by similarity, it follows that:

$$\xi_e = \frac{1}{2H_2|_{opt}} \tag{5.24}$$

This can be used to define the required value of H_2 when designing a TMD for a certain SDOF system. Once the value of the required equivalent damping is deter-

mined, it is possible to find out through the required value of $H_2|_{opt}$ what mass ratio with respect to the mass of the primary system is needed for the TMD. Another required value of the mass ratio of the TMD with respect to the primary system comes from the evaluation of the required amplification factor H_4 for the TMD.

5.2.2 Damped primary systems

An approach similar to the one described above can be outlined for the case of a primary system with damping. Two new amplification functions are introduced, H_5 and H_6 together with a parameter D_3:

$$D_3 = [1-\rho^2][f^2-\rho^2]-\rho^2(\mu f^2-4\xi_d\xi f)+i2(\xi_d(\rho f[1-\rho^2]-\mu\rho^3 f)+\xi\rho[f^2-\rho^2]) \quad (5.25)$$

and the amplification factors:

$$H_5 = \frac{|D_2|}{|D_3|}H_2 \quad (5.26)$$

$$H_6 = \frac{|D_2|}{|D_3|}(1+4\xi^2\rho^2)H_4 \quad (5.27)$$

The displacements have the forms:

$$\hat{u} = -\frac{\hat{a}_g m}{k}H_5 e^{i\delta_5} \quad (5.28)$$

$$\hat{u}_d = -\frac{\hat{a}_g m}{k}H_6 e^{i\delta_6} \quad (5.29)$$

5.3 Extension to MDOF systems

In practical applications the starting point is the definition of the SDOF system to control through the Tuned Mass Damper. In my case the first choice would be to control the first mode. Referring to Table 3.2, the maximum value of the eigenvector

corresponds to the lateral displacement of the midspan node. This is the displacement to control, the displacement can be obtained by superposing the modal contributions. For resonant conditions it is possible to assume that the displacement is function only of the first mode. Calling u^x_{ms} the component of midspan node displacement in the x direction I have the following:

$$u^x_{ms} = \phi^1_{ms} q^1 \tag{5.30}$$

and solving for q^1:

$$q^1 = \frac{1}{\phi^1_{ms}} u^x_{ms} \tag{5.31}$$

substituting in the equation of motion in the form 3.11:

$$\tilde{M} = \frac{1}{(\phi^1_{ms})^2} \tag{5.32}$$

and

$$\tilde{K} = \frac{1}{(\phi^1_{ms})^2} (\omega^1)^2 \tag{5.33}$$

5.3.1 Application to the cable-stayed bridge model

From Table 3.2 it can be seen that the X-eigenvector's maximum value is 4.07501e-04. The value of $1/(\phi^1_{ms})^2$ is 6.02203e+06. As the total mass of the system is: 1.60863e+07, this means that the modal mass of the first mode is 37.40 percent of the total mass. Starting from this and using the optimal parameters and the charts derived by Connor [3], the fundamental parameters of the Tuned Mass Damper to adopt for meeting a certain requirement on the damping added to the system can be derived by defining a performance requirement on the displacements of the primary system at the point in which the eigenvector is maximum. In this case it is the midspan point. Once the optimal mass ratio is defined all the optimal values that

characterize the TMD are chosen. In particular the design is done taking into account a structural damping of 0.02 for the primary system in the first mode.

All the figures used in the following design process are those related to this value of structural damping. The rationale of the design is to use a TMD fine tuned to dampen the first mode in such a way that the amplification factor H_5 will not exceed a fixed value. This is just a partial achievement, as it is related only to a mode, but it is considered a starting point of a certain importance especially in this case, in which the first mode has a frequency which is much higher (0.2940 vs. 0.1287) than the first one in the lateral direction.

Of course there are some limit also in the dimension of the mass to adopt for the damper; in fact in the case of such a large structure the total mass of the system makes the task of damping the amplification of the primary system more difficult. However a starting point will be to design the TMD in a way that the initial gain related to the amount of mass ratio to put in the system is exploited. In fact, observing the plot of $H_5|_{opt}$ versus the mass ratio shown in Figure 5-2, it can be seen how the rate at which the amplification decrease is very fast for a small increase of the mass ratio. In a first dimensioning I chose a value of six for the amplification factor. It can be obtained through a relative low value of mass ratio (3.65 percent).

According to the method here proposed the amplification factor of six for the primary system will bring to certain values of the TMD characteristics that are in particular a mass of $m_d = 223,530Kg$, a dashpot of $c = 40,771Kg/sec$ and a stiffness of $K = 131,190Kg/sec^2$. With this dimensions the TMD amplification factor will be 25.10 and the amplification ratio between the TMD and the primary system 4.18. All this value including the plot of the equivalent damping versus the mass ratio are reported in figures from 5-1 to 5-5. Following these graphs are the results obtained from a simulation on the finite element model under a lateral harmonic load with a frequency equal to the natural frequency of the first mode of the system, and an amplitude of 10,000 KN/m. The static displacement calculated for the system is 0.95 m.

The following cases were considered:

1. primary system without TMD, structural damping of 2 percent,

2. primary system with TMD, with the parameters found with the above method and again a structural damping of 2 percent,

3. finally the system with two TMD both with the same dimension of the single TMD, on both sides of the girder. The structural damping is still 2 percent.

The results in terms of lateral displacements of the midspan point are shown in Figures 5-6, 5-7 and 5-8. It easy to notice how the TMD is effective. In particular the single TMD dampens out the maximum displacement of the primary system to one third of the maximum resonant displacement. Another reduction of the 30 percent is detected when the double TMD is added. This is not a great advantage compared to what was gained in the first step. However, this second applied TMD is interesting and was sufficient for another improvement in the overall performance in the sense the the displacement of the damper is at this level is accepted and almost ready to be implemented See Figure 5-9 to 5-13.

As long as can be shown through this very simple example the efficiency of TMD in passive control systems can be stated. Further analysis could extend to analyze multiple TMD elements in order to keep an effective passive control system on a broader number of loading cases and time histories.

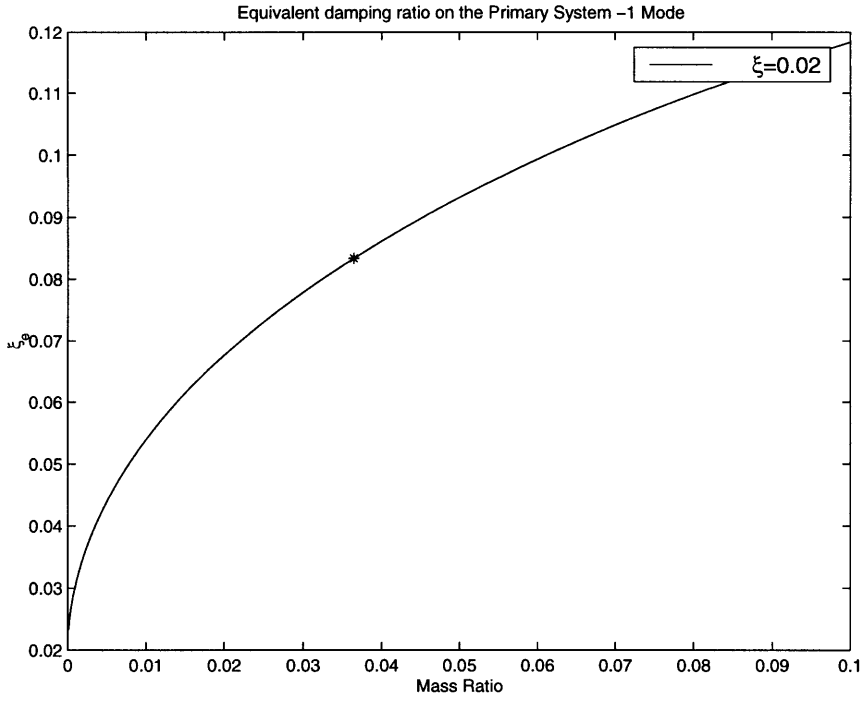

Figure 5-1: Design equivalent damping on the primary system - STMD

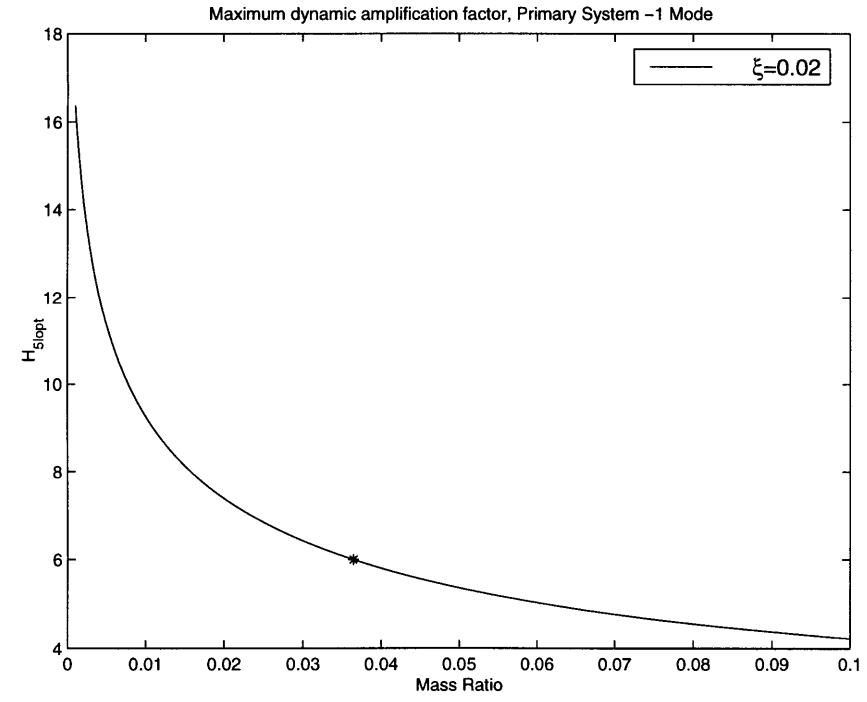

Figure 5-2: Required maximum dynamic amplification factor

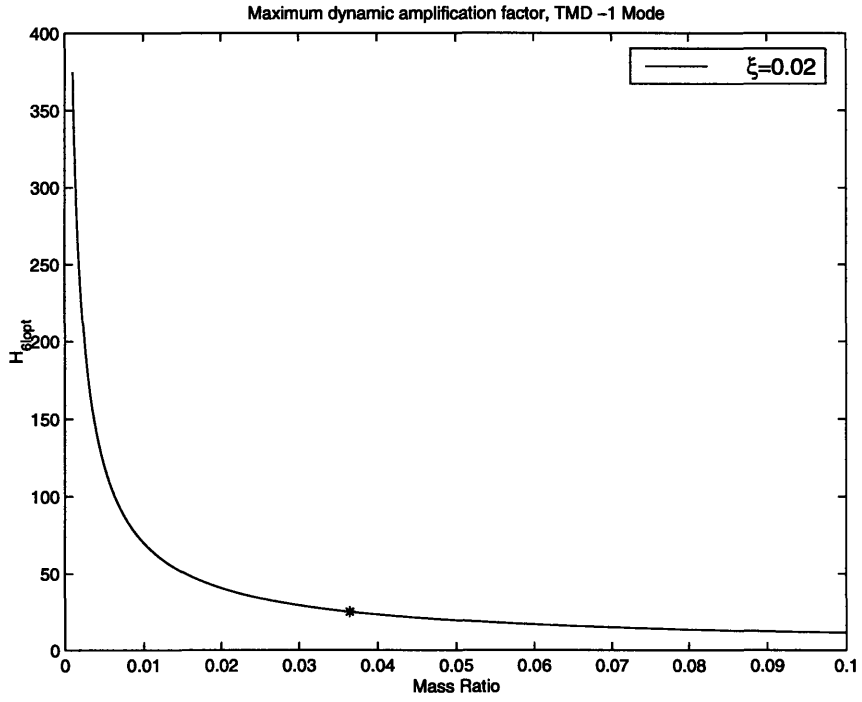

Figure 5-3: Maximum dynamic amplification factor for the damper

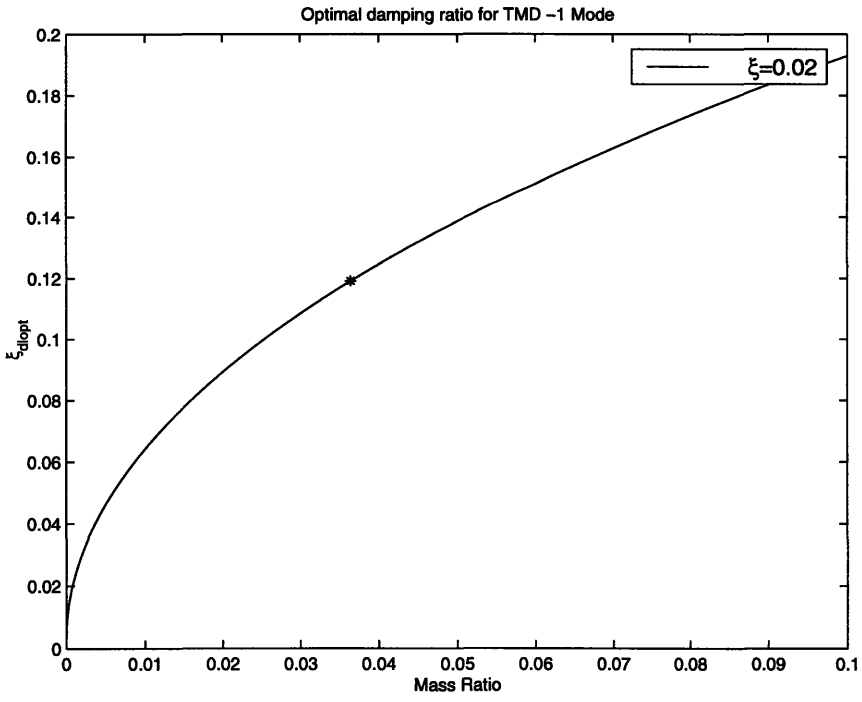

Figure 5-4: Design damping ratio for the dampers - STMD

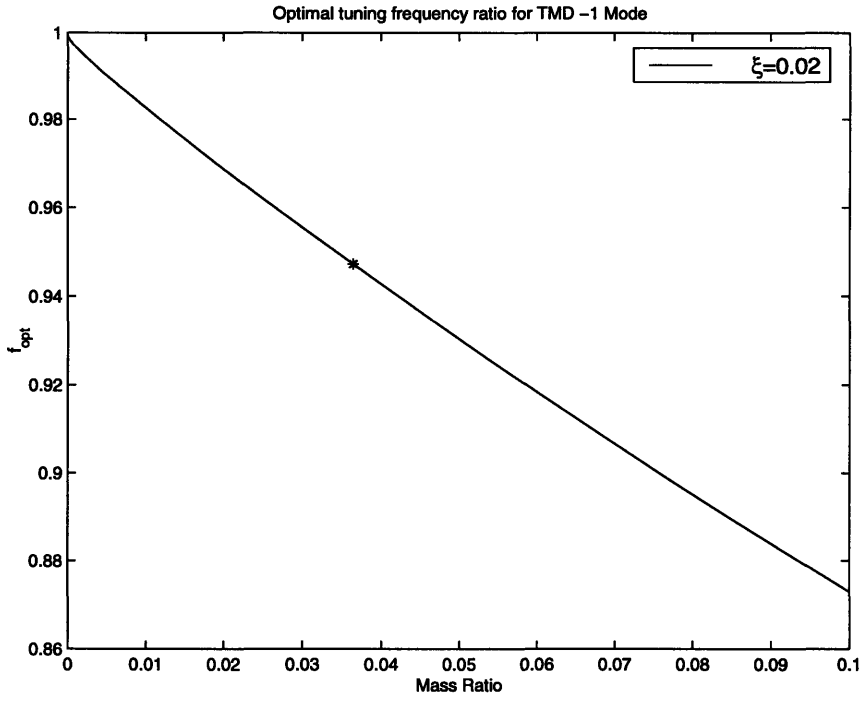

Figure 5-5: Design optimal tuning frequency

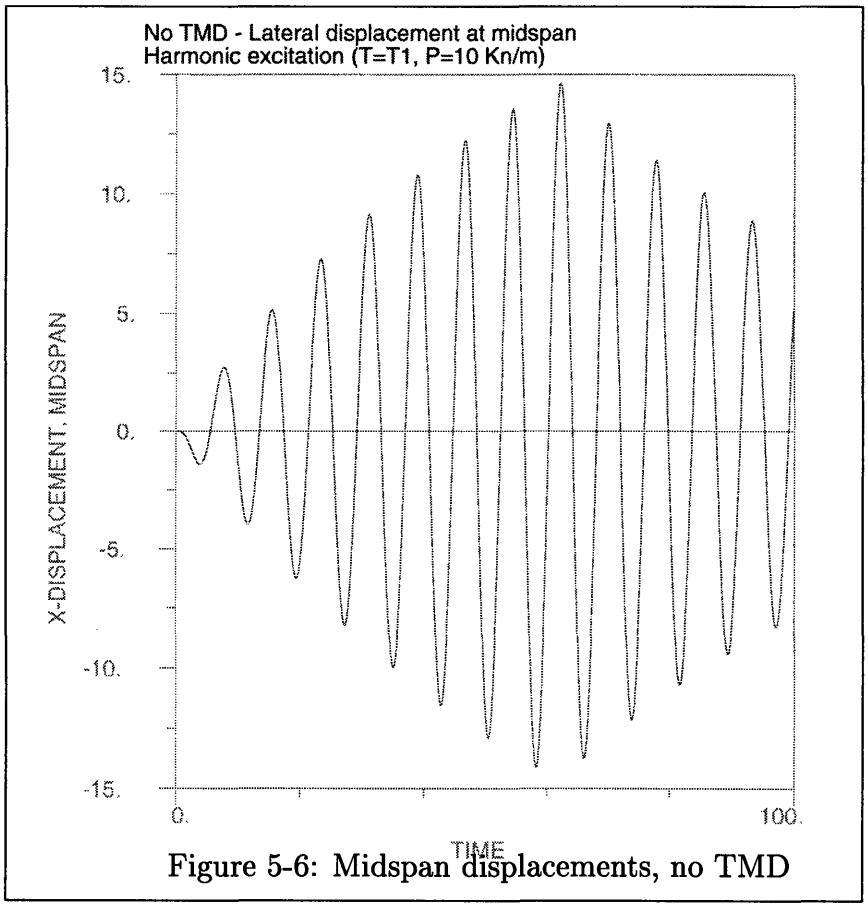

Figure 5-6: Midspan displacements, no TMD

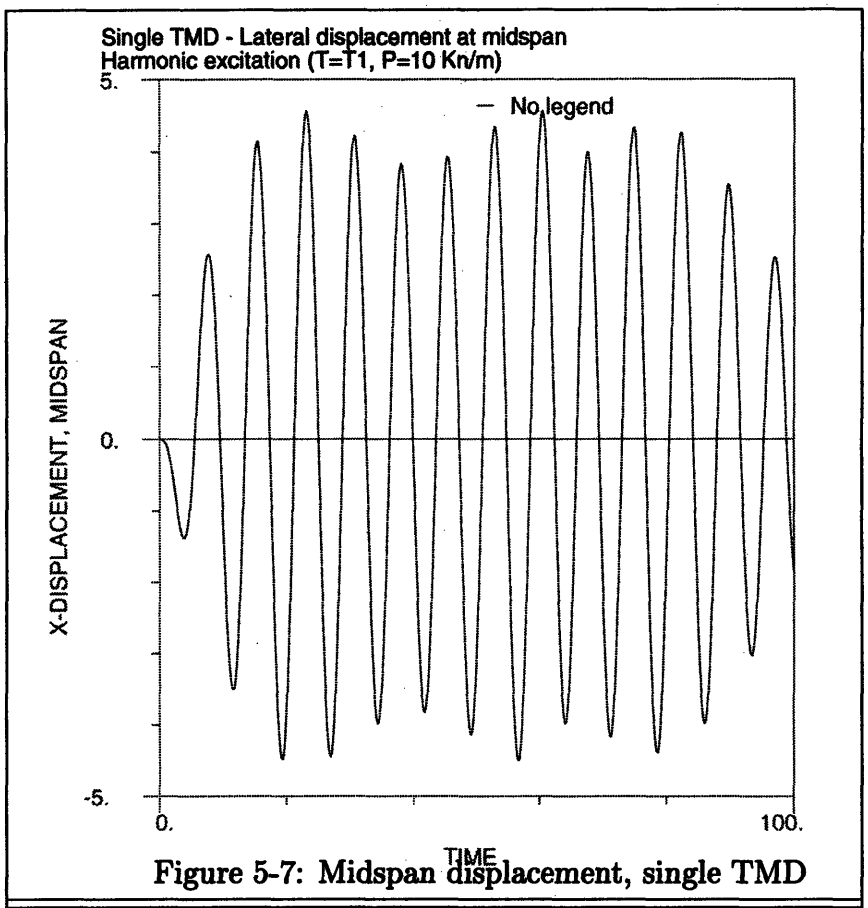

Figure 5-7: Midspan displacement, single TMD

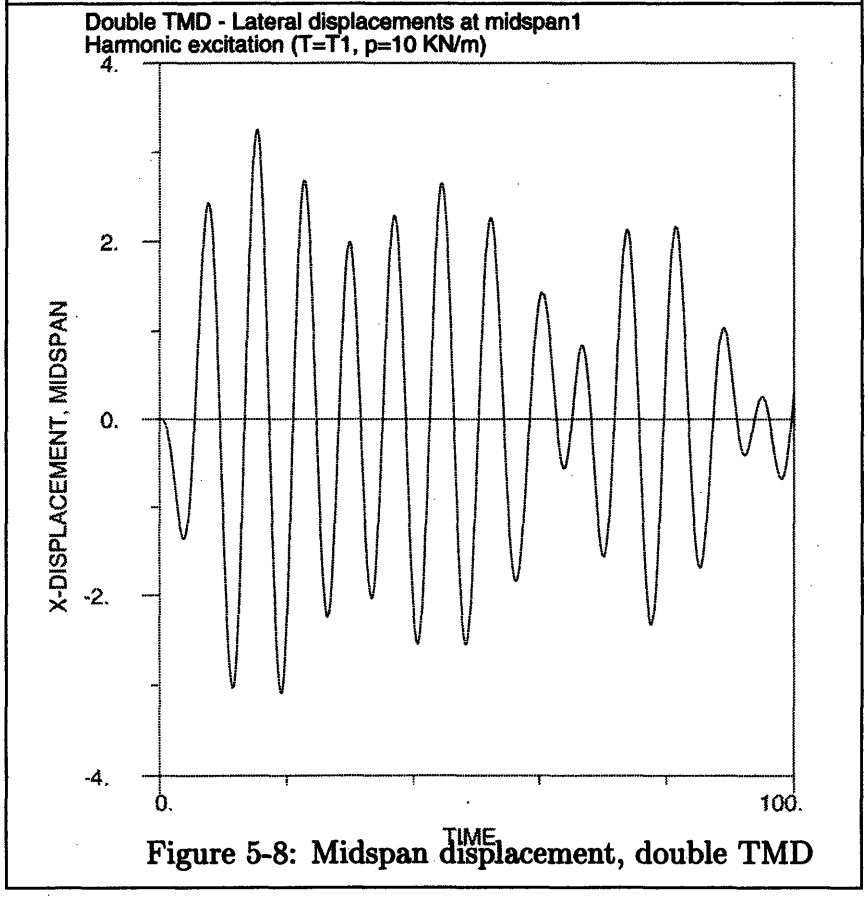

Figure 5-8: Midspan displacement, double TMD

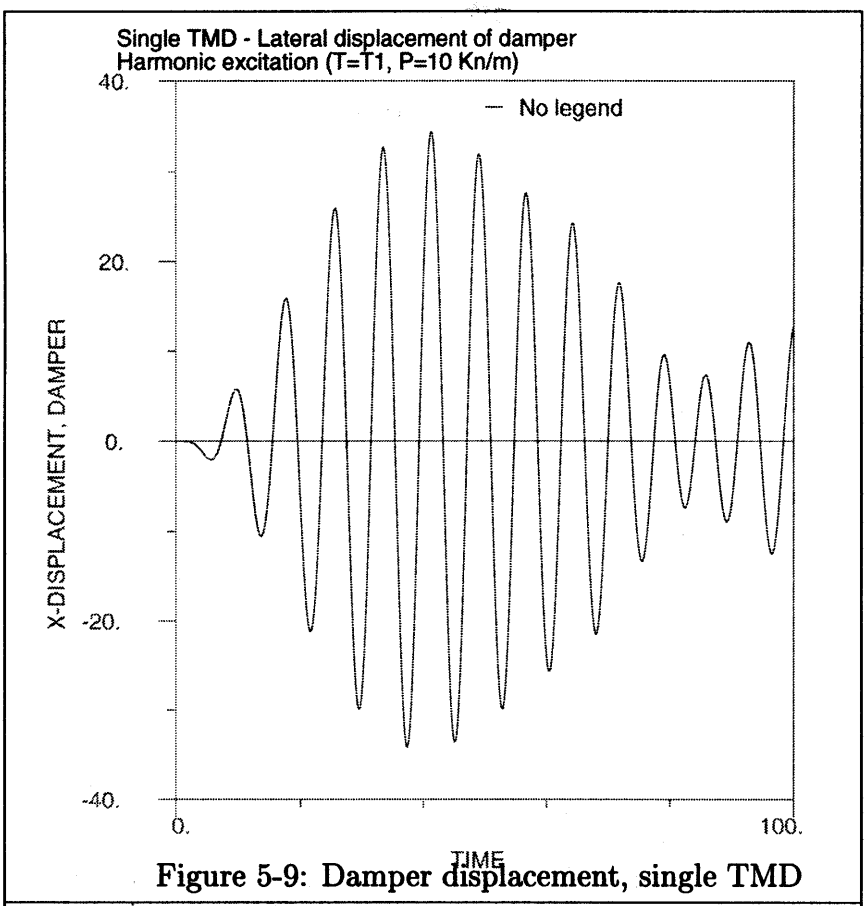

Figure 5-9: Damper displacement, single TMD

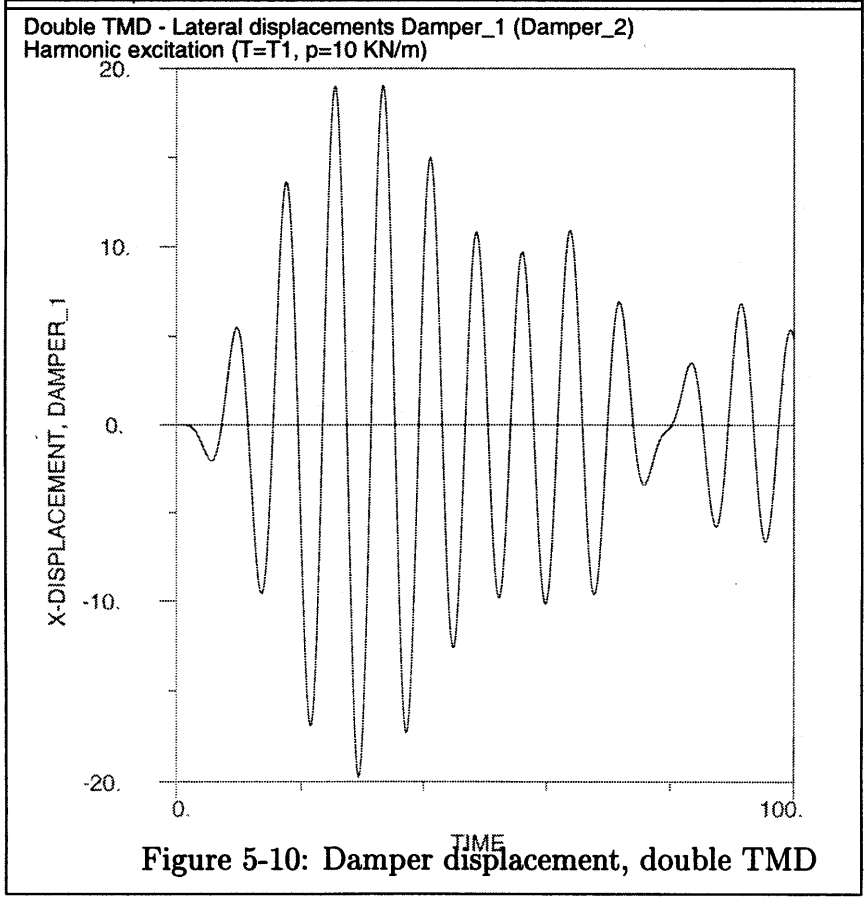

Figure 5-10: Damper displacement, double TMD

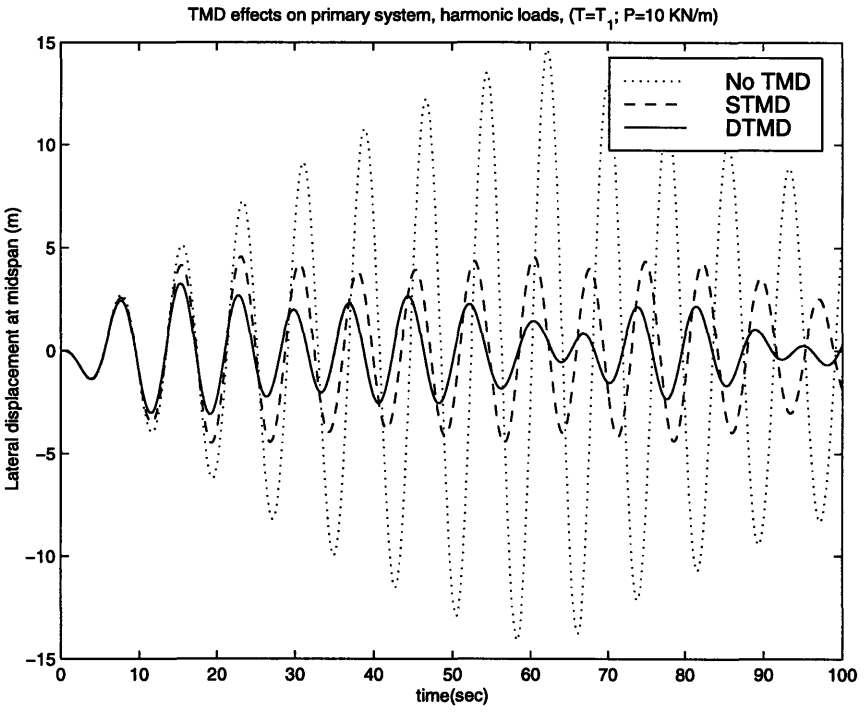

Figure 5-11: Variations on midspan displacements no TMD, single and double TMD

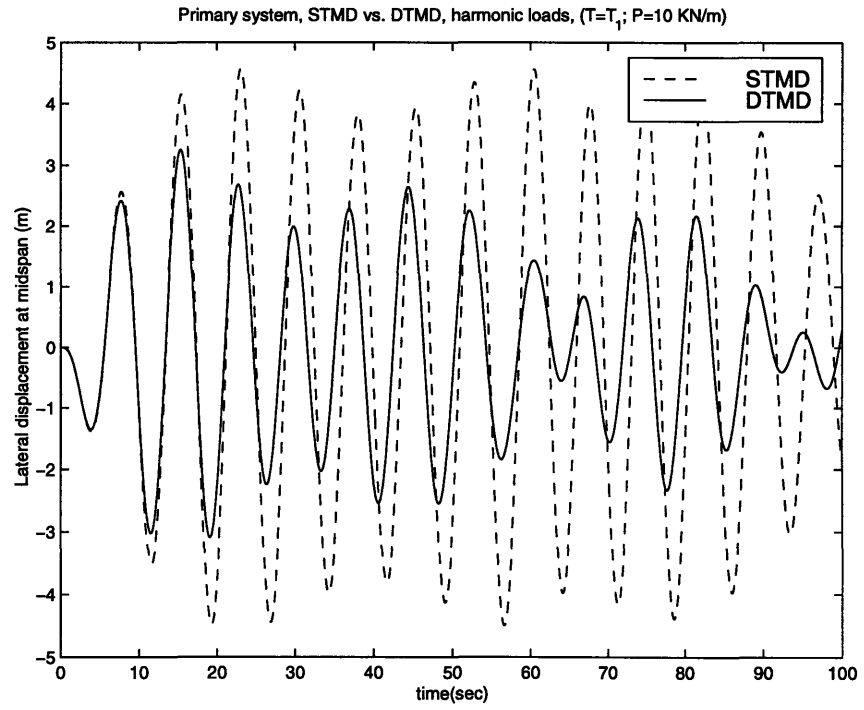

Figure 5-12: Midspan displacement comparison between single and double TMD

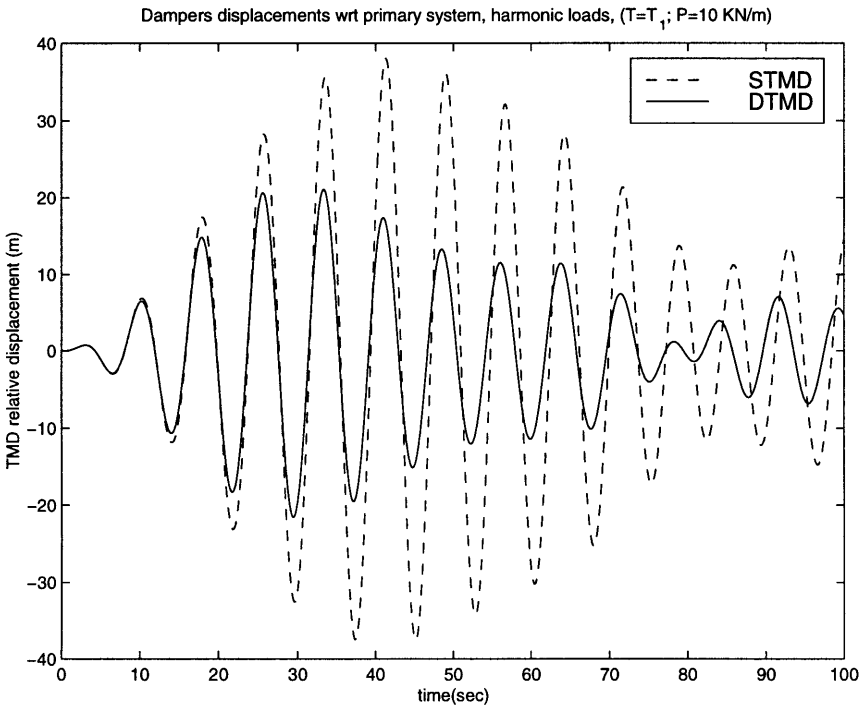

Figure 5-13: Damper vibrations relative to the primary system

Chapter 6

Active motion control systems

In the above chapter a passive systems mostly suited to the control of the resonant effects of wind components forced response was presented. This potential resonance effects of wind are related to the turbulence which is contained in most of the winds actions, the use of damping is one of the most efficient method to deal with undamped and slightly damped structures. On the other hand the active control system is designed to control aerodynamics wind effects on long and super long span bridges. These effects are strongly related to the deformations of the structure itself in a highly non-linear way.

An active control system is defined as a system that actively monitors the motion of a structure and can modify it by means of an actuator powered by an external energy supply. In 6-1 a schematic flowchart provides more detailed information about the concept. The application of active control to civil structures is an innovation that seems economically feasible for long span bridges. The concept of active control, which is broadly applied in the aerospace industry, is still an innovation in civil constructions. Although active control systems have been studied in many projects at the design stage, and on scale models, full-scale systems have been installed on structures only recently and never on bridges by now.

The first applications have been already implemented on buildings, as described in the following paragraphs. The concept of active control can include many different systems even if narrowed down to the construction industry.

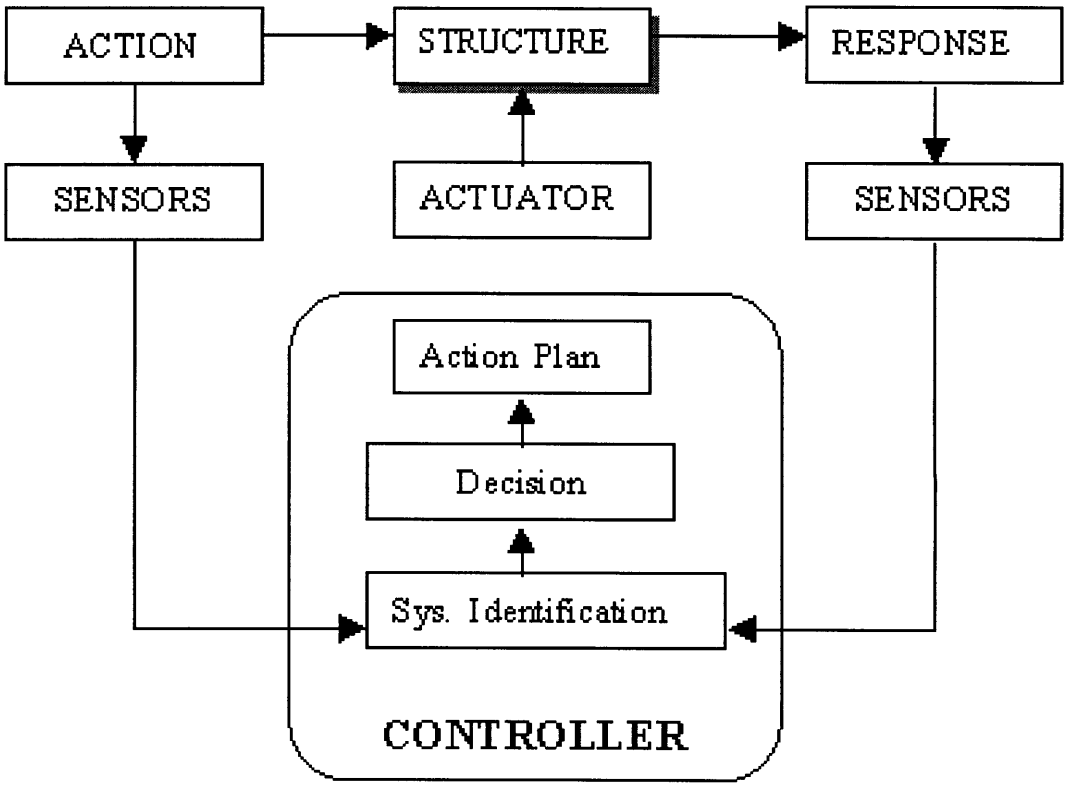

Figure 6-1: Active control flowchart

6.1 Technological paradigms in long span bridge design

The research interest around the topic of bridge aerodynamics has strongly increased after the Tacoma Narrow bridge failure in the 1940. Since then research developed continuously towards safer and more reliable structures. The innovation has been mostly incremental and the development has mainly been in design and in material technology. The technology transfer from the aircraft industry has influenced the innovation: wind tunnel tests have been used more often and have brought new concepts in the design of optimally streamlined sections. The latest evolution has been characterized by modular innovations such as the adoption of new materials and of particular devices and design solutions aimed to reduce dynamic effects and vibrations.

As new high-strength materials are adopted for cables and other structural elements the aerodynamics wind effects related to structural flexibility are the main limit towards the construction of super long spans. In fact, the evolution is towards lightweight structures with high material stresses and for which the performance requirements for deformations control the design and construction choices. The high cost of high-strength materials is only affordable if an optimal material distribution throughout the structure is achieved. Active control systems adopted to control the motion of a structure can reduce the materials' quantities otherwise needed in the construction. These systems can therefore be conceived as common element in wind sensitive bridge to increase the comfort of the users, to reduce the fatigue damages, and as a result of this, to increase the safety of the structure on a long term basis.

6.2 Technical description and background

At the moment in bridge engineering effective applications of active control are thought and applied to the control of wind actions more than to the control of seismic excitations. In fact, as the earthquake excitation is impulsive, short time lags

between the time in which the external signal is detected and the time in which the countermeasure is taken can easily undermine the efficiency of the system.

The innovation presented here is based on the idea of using of control surface on the side of a bridge deck to control the aerodynamic response of long span bridges to extreme wind conditions [17]. The system here presented has been developed by COWI, a medium size danish design and construction management firm highly specialized in bridge engineering and aerodynamics. The innovation is based on the idea of constantly monitoring the movements of the deck and on the use of control surfaces movements to generate stabilizing aerodynamic forces counteracting any tendency to movement. This will bring an increase of the critical wind speed up to 50 percent.

The control surfaces are airfoils of polyurethane foamed stainless steel sheeted sandwich. Because of their lightness they can easily be supported at a distance of 5-10 m symmetrically on both sides of the bridge deck. Control rods activated by hydraulic cylinders, with short time rise, operate the airfoils. The hydraulic cylinders are activated by means of computer controlled servo pumps. The computer operates on the basis of signals from accelerometers located in the bridge girder, in accordance with a service function developed on the basis of mathematical modeling and wind tunnel tests.

Bridge engineering firms specialized in design and construction of long span structures have to develop high-end technologies to compete in a very tight market which is based on low-cost bids or distinctive-capabilities competitions. The advantage of the presented innovation is that it can be easily applied to a different range of projects.

The implementation of this innovation in bridge construction is affordable as great part of this technology is derived and adapted from aircraft industry; the advantage is that adequate system reliability can be accomplished by adopting standards already in use in that industry. This will still be an innovation when designed for and applied to civil engineering systems but at the mean time can be upgraded on the basis of already developed research and design paradigms. In a similar way the innovation can take advantage from the enhancements achieved in the computer industry particularly in the area of data storage and processing.

6.3 Stage of development

To define the potentiality of the described innovation it is very beneficial to investigate what is the state of the art in the field of applications of active control to construction. This process is still in a pre-paradigmatic design phase [21], in which on the one hand there is a strong push for research and developing of new technologies, on the other hand the application of innovations to the construction world are still in a pioneering age.

The evolutionary development of a branch of science is usually developed from a pre-paradigmatic stage during which a body of theory reaches its maturity, to a paradigmatic stage in which dominant patterns emerge and evolve toward design and implementation. The technological paradigm [6], of active control has been developed under the technology push of the aerospace industry and have recently taken advantage of the progress of computer industry and material science. Design and construction companies, operating in the area of highly specialized structure are developing their own paradigms trying to gain a competitive advantage from being the first innovators in their specialties, their objective is to define what can be the dominant design of the future.

The first application of actively controlled structures has been implemented in buildings in Japan [3]. Kajima Corporation has pioneered the field with the Kyobashi Seivan, an eleven stories building in Tokyo equipped with an Active Mass Damper (AMD) on top of it. The purpose is the limitation of motion response to lateral loads. The AMD is activated when the sensors embedded in various part of the structure send a signal to the processors that exceed a fixed limit. In this case the processors send a feedback to an actuator that applies a force sufficient to start the mass of damper. The efficiency of the system has been measured in the capability of reducing the uncontrolled response to one third. A more recent application is the Nishikicho Building a fourteen stories building whose construction was completed in 1993 in Japan. The system is conceptually similar to the former the only difference being that the AMD is coupled to a Tuned Mass Damper (TMD), which is a passive device.

The AMD is activated by a an active system of sensors, processor and actuator, its mass is much smaller than the TMD mass and the purpose is to dampen out the oscillation of the TMD through the use of a smaller force.

The extension of the application to bridge design is more difficult as the forces and the masses involved are much larger than in the described buildings. However the COWI innovation, as continuously distributed along the structure does not require the activation of large masses or forces. As the core part of the system is in the triangle sensor, processor/controller, actuator, the observation of existing systems installed on buildings has been highly beneficial to the innovation.

The application of active control to bridge construction can potentially bring a nontrivial change in the field of long span and super long span bridges. Although derived from the aerospace industry and developed and applied to building construction industry, its implementation to the bridge construction industry is completely new.

The described application of active control to bridge design and construction is a system innovation; its integration into a new bridge improves the structural performance of the system. In fact, the introduction this subsystem into a bridge completely changes the concept of the analysis and the behavior of the entire system is completely changed. Furthermore, the embedded system that continuously collects data during the life cycle of the structure, increases the possibility of following the state of the structure without time consuming and expensive inspections. An extension of the system is the application to existing structures suffering from excessive deflections due to the interaction with the aerodynamics effects of wind.

The system is based on the collection of data of the response of the structure to an external action. At the same time the external excitation (i.e.; the wind action) is measured and the data are stored, these two set of data will serve as a powerful tool to identify the system characteristics through the analysis of the response.

The direct consequence of this is that this system plays the double role of actively controlling the structure and providing a series of data along the life cycle of the structure. These data can help in keeping track of the status of the system and consequently decide if the structure is still meeting the performance requirements for

which it was originally designed. This follows the trend in structural monitoring that is moving towards installing equipment able to keep track of the behavior of new structures all through their life cycle.

6.4 Future potentiality

The active flutter control system has been proposed for a patent; it has the potentiality for becoming a dominant paradigm in the design and construction of long and super long span bridge. In fact, the full exploitation of the system could create new opportunities in the area of super long span bridges by increasing the technical and economic feasibility of many projects whose feasibility has been considered for a long time such as the Africa/Europe Gibraltar crossing, the Bering Strait crossing, the Messina Strait crossing.

The advantage from an economical point of view is much greater as the span increases; in fact, the cost of material needed for the uncontrolled structure to meet the required performance increases exponentially with the span. As a consequence, the benefits that could come from the introduction of this innovation will come mostly from projects in a span range over 1,000 m for cable-stayed bridges and over 2,000 m for suspension bridges. That is considered the scenario of the future. At the same time the application of the active control system to existing bridges can be adopted for facilities that show sensitivity to aerodynamics effects of wind at any time during their life cycle. This area is continuously expanding in an age in which the government investment for rehabilitation and retrofitting of existing infrastructure facilities is growing fast compared to the investment for new constructions [18].

An efficient control system can improve the technical/economical feasibility of large projects. Moreover, a system that provides a total control on the behavior of a structure during its life cycle will increase the safety of the users of the facility. Last but not least if less materials are involved in the construction, the environmental sustainability of a structure is improved. The implementation of this innovation in a new or an existing bridge can establish a dominant design, particularly in the area of

super long span bridges. The conclusion is that the full exploitation of this innovation can bring great benefits to design and construction of new long-span bridges. Further advantages from the development of the described innovation should come up when transferring it to active control of earthquake excitation.

Chapter 7

Conclusions

The objective of my thesis has been the identification of some of the most relevant issues in the design of long-span cable-stayed bridges. This type of structures has recently experienced an interesting evolution and it seems that the limit span is going to increase in the next future.

The idea of a design that mostly relies on the high tension capacity of new materials is very powerful when coupled with a performance-based design. The simplified proposed method presented here is a potential new approach to design of very flexible structures and is mostly focused on the overall deformation performances of the structural system.

This first step, together with more development of passive and active devices for control of structural motion, could lead to new achievements in cable-stayed bridges design. It is possible to think of structure that will perform better in their whole life-cycle. The higher safety and serviceability performance will be the basis for the design of these large structures.

The analysis of the approach to the design of Tuned Mass Dampers has shown that good results can be achieved through simplified design that again is based on the motion based requirement for the structure.

An analysis of the main phenomena related to wind-structure interaction has been also addressed. This is the basis for the design of structures that meet their performance requirements under the excitation due to strong wind.

Great impulse to wind engineering will come from a more unified approach to the problem of the aeroelastic interaction between wind and structure. Strong improvement to the field could easily come from the increased power of computational tools and from the progress in the field of computational fluid dynamics.

Bibliography

[1] K. J. Bathe and A. P. Cimento. Some practical procedures for the solution of nonlinear finite element equations. *Computers Methods in Applied Mechanics and Engineering*, 22:59–85, 1980.

[2] K.J. Bathe. *Finite Element Procedures.* Prentice Hall, Englewood Cliffs, USA, 1996.

[3] J. J. Connor and B. S. A. Klink. *Introduction to Motion Based Design.* Computational Mechanical Publications, Southampton, UK, Boston, USA, 1996.

[4] ADINA R & D. Adina, theory and modeling guide. Technical Report 95-8, ARD, 1995.

[5] J. P. Den Hartog. *Mechanical vibrations.* John Wiley and Sons, New York, 1940.

[6] G. Dosi. Technological paradigms and technological trajectories. *Research Policy*, 11:147–162, 1982.

[7] J. H. Ernst. Der 'e-modul' von seilen unter beruckisichtigung des durchhangs. *Der Bauingenieur*, 40(2), 1965.

[8] J. F. Fleming. Nonlinear static analysis of cable-stayed bridge structures. *Computers and Structures*, 10:621–635, 1979.

[9] J. F. Fleming and E. A. Egeseli. Dynamic behaviour of cable-stayed bridges. *Earthquake Engineering and Structural Dynamics*, 8:1–16, 1980.

[10] N. J. Gimsing. *Cable supportde bridges: concept and design.* John Wiley and Sons, 2nd edition, 1997.

[11] M. Hetenyi. *Beams on elastic foundation; theory with applications in the fields of civil and mechanical engineering.* University of Michigan studies. Scientific series; v. 16. The University of Michigan press, 1946, 1946.

[12] F. Leonhardt and W. Zellner. Past present and future of cable-stayed bridge. In M. Ito, editor, *Cable-Stayed Bridges, Recent Developments and their Future*, pages 1–33, The Netherlands, 1991. Elsevier.

[13] A. S. Nazmy and A. M. Abdel-Ghaffar. Non-linear earthquake-response analysis of long span cable-stayed bridges: Theory. *Earthquake Engineering and Structural Dynamics*, 19:45–62, 1990.

[14] A. S. Nazmy and A. M. Abdel-Ghaffar. Non-linear earthquake-response analysis of long span cable-stayed bridges: Applications. *Earthquake Engineering and Structural Dynamics*, 19:63–76, 1990.

[15] C. O' Connor. *Design of Bridge Superstructures.* John Wiley and Sons, New York, 1971.

[16] M. Ohashi. Cables for cable-stayed bridges. In M. Ito, editor, *Cable-Stayed Bridges, Recent Developments and their Future*, pages 125–150, The Netherlands, 19916. Elsevier.

[17] Larsen A. Ostenfeld K. H. Bridge engineering and aerodynamics. In Larsen A., editor, *Aerodynamics of Large Bridges*, Rotterdam, 1992. Balkema.

[18] G. Seaden. Economics of innovation in the construction industry. *Journal of Infrastructure Systems*, 2(3):103–107, 1996.

[19] S. P. Seif and W. H. Dilger. Nonlinear analysis and collapse load of p/c cable-stayed bridges. *Journal of Structural Engineering, ASCE*, 116(3):829–849, 1990.

[20] E. Simiu and R. H. Scanlan. *Wind effect on structures.* John Wiley and Sons, New York, 1986.

[21] D.J. Teece. Profiting from technological innovation: Implication for integration, collaboration, licensing and public policy. *Readings in the Management of Innovations*, pages 621–647, 1987.

[22] M.S. Troitsky. *Cable-stayed bridge: Theory and design.* BSP Professional Books, London, 1988.

[23] R. L. Wardlaw. Cable supported bridges under wind action. In M. Ito, editor, *Cable-Stayed Bridges, Recent Developments and their Future*, pages 213–234, The Netherlands, 1991. Elsevier.

[24] J. C. Wilson and Gravelle W. Modeling of a cable-stayed bridge for dynamic analysis. *Earthquake Engineering and Structural Dynamics*, 20:707–721, 1991.